The isohydric strategy of Platanus x hispanica tree shapes its response to drought in an urban environment

Alice Claude, Paul Nadam, Ludvine Brajon, Luis Leitao, Séverine Planchais, Valentin Lameth, Jean-françois Castell, Younès Dellero, Arnould Savouré, Anne Repellin, et al.

The isohydric strategy of *Platanus × hispanica* tree shapes its response to drought in an urban environment.

Alice Claude[1], Paul Nadam[1], Ludvine Brajon[2], Luis Leitao[1], Séverine Planchais[2], Valentin Lameth[1], Jean-François Castell[3], Younès Dellero[4,5], Arnould Savouré[2], Anne Repellin[1], Juliette Leymarie[1#*], Ruben Puga Freitas[1#]

[1] Univ Paris Est Creteil, CNRS, Sorbonne Université, INRAE, IRD, IEES-Paris, Institut d'Ecologie et des Sciences de l'Environnement de Paris, F-94010 Créteil, France
[2] Sorbonne Université, Univ Paris Est Creteil, INRAE, CNRS, IRD, Institute for Ecology and Environmental Sciences of Paris, iEES Paris, F-75005, Paris, France
[3] UMR 1402 Ecosys, AgroParisTech, 22 place de l'Agronomie, 91120 Palaiseau
[4] INRAE, Université Rennes, Institut Agro, IGEPP-UMR1349, Le Rheu, 35653, France
[5] P2M2, MetaboHUB-Grand-Ouest, France
# These authors contributed equally to the article

***Corresponding author:**
Juliette Leymarie,
Email : juliette.leymarie@u-pec.fr

Funding

This work benefited from the French national research agency (ANR) via the sTREEt (Impact of STress on uRban trEEs on ciTy air quality) project (grant no. ANR-19-CE22-0012). Ludvine Brajon benefited from Master Internship grant from IEES-Paris.

Edited by Y. Utsumi

Abstract

Urban vegetation provides many ecosystem services like heat island mitigation. However, urban trees are subjected to the stresses that they are meant to alleviate, with drought being a main constraint. We investigated the drought response strategy of plane trees (*Platanus* × *hispanica*), focusing on stomatal regulation and metabolic remodelling. To address this question, a semi-controlled experiment was performed in an urban site with fourteen plane trees grown in containers. From May to June 2022, those trees were physiologically characterized in response to a controlled edaphic drought completed by a targeted metabolome analysis focused on amino acids, sugars, polyols and organic acids. Early *P.*

× *hispanica* response to drought consisted in stomatal closure limiting carbon assimilation and osmotic adjustment, which was likely related to malate and trehalose accumulation. Both allowed the maintenance of stem water potential and Relative Water Content. As the drought became severe, when the extractable soil water content (eSWC) dropped below 30%, a non-stomatal limitation of photosynthesis was observed and was associated with photosynthetic apparatus damage (reduced chlorophyll content and decrease in F_v/F_m) and a further decline in carbon assimilation. When eSWC decreased below 25%, severe drought induced defoliation. Together, these results highlight the isohydric strategy of *P. × hispanica*, based notably on osmotic adjustment and explain its resistance to drought combined with other urban constraints. In the context of climatic change in cities, it would be interesting to analyse the impact of successive drought cycles in the long term, aiming for sustainable planning and management of urban trees.

1 Introduction

Vegetation in urban areas is widely acknowledged as a source of many ecosystem services. These services include mitigating the heat island effect, reducing air pollutants, storing carbon, managing water runoff, promoting biodiversity, and enhancing the well-being of city inhabitants (Roy et al. 2012; Larondelle and Lauf 2016). However, urban forests and urban trees, particularly, are also subjected to the stresses that they are meant to alleviate (Calfapietra et al. 2015; Barradas and Esperon-Rodriguez 2021). Indeed, cities are often described as 'heat islands' and may be characterized by poor air quality and limited space for root growth and canopy expansion. Thus, urban trees are prone to both atmospheric and soil drought stresses, conditions that are inciting and contributing factors leading to enhanced tree mortality, notably during the establishment phase corresponding to the first five years post-planting (Roman and Scatena 2011; Lawrence et al. 2012; Hilbert et al. 2019; Czaja et al. 2020). In addition, climate change increases the vulnerability of urban trees, with recent estimates suggesting that 50% of these tree species are currently beyond their 'safety margin' (Esperon-Rodriguez et al. 2022). This study classified *Platanus* species as out of their safety margins in several European cities, mainly in relation to the lack of precipitation (*P. occidentalis*) and high temperature (*P. orientalis*). Trees belonging to the genus *Platanus* are common in many cities worldwide; *Platanus* × *hispanica* is among the most planted species in cities across Europe, including the Mediterranean regions (Tattini et al. 2015) and it is also prevalent in cities in Australia (Sanusi and Livesley 2020), Japan (Tan et al. 2021), China (Ju et al. 2017) and in the USA (Sherman et al. 2016). According to the Paris trees database (https://opendata.paris.fr; data April 2023), 18% of the trees inventoried and 38% of street trees are London plane trees. Indeed, many plane trees are found in street alignments, where they are exposed

to high pollution levels and restricted growing spaces and water supply. The hybrid *Platanus* × *hispanica* (also known as *Platanus × acerifolia*, London plane, or common plane), a cross between *P. occidentalis* and *P. orientalis*, is generally identified using morphological parameters. However, molecular tools are recommended for precise species identification, notably to differentiate the hybrid from its parent species (Lang 2010; Rinaldi et al. 2019; Besnard et al. 2022). Until recently, plane trees have exhibited stress resilience under urban conditions (Tello et al. 2000; Sanusi and Livesley 2020; Paris city 2023), some of them becoming heritage trees. Despite the sensitivity of *P.* x *hispanica* to canker stain (*Ceratocystis fimbriata platani*) and recent efforts to diversify urban tree populations, plane trees remain highly popular among green space planners. Generally, young trees are quite susceptible to the harsh urban environment, notably during their first years post-planting (Sherman et al. 2016). Given that drought is identified as the main inciting and contributing biophysical factor to urban tree mortality (Whitlow et al. 1992; David et al. 2018; Hilbert et al. 2019), it is essential to improve knowledge on the responses of young plane trees to water limitation. Several studies carried out on adult urban trees have shown that *P.* × *hispanica* displays moderate drought tolerance to water deficit, based on the analysis of growth parameters (Gillner et al. 2015; Gatto et al. 2021; Hirsch et al. 2023). To date, only three studies report on the response mechanisms to drought of containerized young *Platanus* × *acerifolia* hybrid trees, with contradictory conclusions regarding their water-saving strategy. While isohydry characterized the overall response to water stress of two-year-old plane trees grown in 20 L containers (Tattini et al. 2015), 4-6 years old plane trees planted in 50 L containers and exposed to reduced water supply were qualified as anisohydric (Dervishi et al. 2023; Rahman et al. 2023). To address the knowledge gaps on *Platanus* responses to drought, our study focused on seven-year-old plane trees (*P.* × *hispanica*) suitable for street planting as alignment trees but still small enough to be containerized to facilitate the control of water supply. To mitigate some limitations associated with container-grown trees (Rahman et al. 2023), large containers (500 L) were used. Furthermore, to mimic urban conditions accurately, the experiment was conducted outdoors in an urban environment near Paris, France, where uncontrolled air quality, pathogen attacks and heat waves were combined. The aim of this study was to exhaustively characterize urban plane tree responses to imposed edaphic drought using morphological, physiological and biochemical parameters and their interplay. In particular, we tested whether stomatal regulation and metabolic remodelling contributed to an isohydric strategy in *P.* × *hispanica*. In addition, the application of an extended period of drought allowed us to characterize severe stress responses in plane trees.

2 Materials and methods

2.1 Plant material and experimental setup

Fourteen plane (*Platanus* × *hispanica*) trees were grown individually in black containers placed on wooden pallets lying on black asphalt pavement in the city of Vitry-sur-Seine, France (48° 46' 36" N, 2° 22' 32" E) (Fig. S1). The five-year-old trees (4 m high) were provided by the tree nursery of "Ville de Paris" (Achère la Forêt) in February 2020. They were planted in 500 L-containers (truncated cones, lower diameter: 0.8 m, upper diameter: 1m, height: 0.8 m) filled with a substrate commonly used by the Green Spaces Unit of "Ville de Paris" (Fig. S1f). In the courtyard, the pots were organized in two rows (trees 1-7 A and 1-7 B) oriented east to west. They were equipped with total rainfall exclusion systems. Before the application of the drought treatment, trees were watered one to three times per week, depending on the weather conditions. Between May 16 and June 17 2022 (*i.e.* for 29 days), seven of the 14 trees were subjected to controlled drought by water withholding. These trees had already experienced a moderate drought imposed by water withholding in 2021. Trees 7A and 7B were used for destructive or disturbing measurements (to establish the models for the determination of leaf projected area and leaf chlorophyll content). The other 12 trees represented six biological replicates for each watering treatment (drought and control treatments).

2.2 Meteorological parameters and soil water content

At the study site, meteorological data were measured every ten seconds at a height of 2 m. Air temperature and humidity were measured with a HMP45A thermohygrometer (Vaisala), Photosynthetically Active Radiation (PAR) was quantified with a Li-190 PAR quantum-meter (LI-COR). Data recorded with a CR1000 datalogger (Campbell Scientific) were averaged over ten-minute-periods and are available online (DOI: 10.5281/zenodo.12742190). Weekly, the water content of the potting soil was determined from a core bored vertically over the entire vertical profile, using a soil core sampler. Small volumes of soil (~ 0.03 L) were collected every 10 cm at depths of 20-50 cm. For each depth, fresh samples were weighted (FW) and oven-dried for one week at 60°C, to obtain their dry mass (DW). Soil gravimetric water content (SWC) expressed as the mass of water per mass of dry soil ($g_{H20}\ g_{soil\ DW}^{-1}$) was calculated as: (FW-DW)/FW and then expressed as extractable Soil Water Content (eSWC), using the previously determined available water capacity of 0.68 $g_{H20}\ g_{soil\ DW}^{-1}$.

2.3 Genotyping of plane trees

DNA was extracted from leaf samples collected from the young plane trees and from reference trees using the CTAB method (Doyle and Doyle 1990). The reference trees were hybrid planes *Platanus* × *hispanica* and trees belonging to the parent species of the hybrid planes, *i.e. Platanus occidentalis* and *Platanus orientalis.* Reference trees were found at French national botanical gardens, the 'Jardin des

Plantes' in Paris and the 'Arboretum de Versailles-Chèvreloup' (Muséum National d'Histoire Naturelle, France; Table S1). Genetic diversity was analysed using 10 microsatellites markers, according to Lang (2010) and Rinaldi et al. (2019) (Table S2) after PCR amplification with DreamTaq polymerase (ThermoFischer Scientific), using 10 ng of template DNA. The PCR program was initiated at 94°C for 3 min, followed by 35 cycles at 94°C for 30 s, 61°C for 30 s, 72°C for 1 min, and a final elongation of 7 min at 72°C. The amplified products were analysed at the genomic platform of the « Institut Mondor de Recherche Médicale » in Créteil (France) with a Seq Studio genetic analyser. The amplicon size analysis was performed using a microsatellite analysis software (Appliedbiosystems®: Microsatellites).

2.4 Allometry measurements

At the beginning of the experiment, branches (one per tree) located at similar heights were selected. Every two weeks, the number of leaves per branch, the length of their major vein, and their physiological state (levels of chlorosis, necrosis, yellowing and presence of *Corythucha ciliata)* were visually evaluated and recorded. Chlorosis corresponded to the presence of localized bleaching due to lace bug bites, necrosis to localized brown leaf surfaces and yellowing to an overall yellowish foliar coloring. Individual leaf lifespan and leaf production were monitored by tagging leaves with colored threads. The leaf projected area was predicted from the vein length data, using the model described in Fig. S3.

2.5 Ecophysiological parameters

The ecophysiological measurements were performed on leaves located in the middle of the tree canopy (ca. 2 m above the base of the trunks).

2.5.1 Stem water potential

Once a week, stem water potential (Ψ_{stem}) was measured at around 14:00 local time using a PMS1000 Scholander pressure chamber (PMS instrument Co.). One leaf per tree was dark-acclimated in aluminium foil for at least two hours before the measurement to allow equilibrium between the leaf and stem water potentials (Naor 1998; Agliassa et al. 2021; Blanco et al. 2021). The equilibrated leaves were cut at the base of the petiole with a razor blade and quickly enclosed in the pressure chamber, with the petiole section protruding. The pressure inside the chamber was gradually increased (0.03 MPa s^{-1}) until xylem sap moistened the petiole section. At this point, the pressure inside the chamber was recorded and corresponded to the opposite of Ψ_{stem} (MPa).

2.5.2 Leaf relative water content

Leaf Relative Water Content (RWC) measurements were carried out once a week (except on week 22) on 5 leaf discs taken from the upper part of the canopies. The total fresh mass of these 5 discs was weighed (FW), then they were placed on distilled water with the abaxial side on water surface, at 4°C during 6 h in the dark, until fully turgid. The turgid weight (TW) of the discs was measured and their dry weight (DW) was obtained after 48 hours in an oven at 60°C. The RWC was calculated according to the following formula: RWC (%) = (FW − DW) / (TW − DW) * 100 (Barrs and Weatherley 1962).

2.5.3 Gas exchange and chlorophyll fluorescence measurements

Leaf gas exchanges were measured using a portable infra-red gas analyser CIRAS 3 (PPSystems) coupled to a CFM-3 light and chlorophyll fluorescence module. Air flow entering the cuvette was set to 300 mL min^{-1}, with a constant CO_2 concentration of 410 ppm, a water vapor partial pressure of 1.5 kPa and leaf temperature maintained at 25°C. Light intensity was set to 1000 $\mu mol.m^{-2}.s^{-1}$ PPFD. Measurements were taken when both A, G_s and Ci were stable, generally three min after leaf insertion in the cuvette. They were repeated on three different leaves per tree.

Stomatal conductance of the abaxial leaf surface was measured using an AP-4 leaf porometer (Delta-T) at ambient temperature and light conditions, following the manufacturer's instructions. Three leaves (those used for gas exchange measurements or the nearest) were considered on the same branch and five measurements were taken per leaf and were measured multiple times during daylight hours.

Maximal quantum yield of Photosystem II (PSII) was measured with a PAM 2500 fluorimeter (Walz) on leaves that were dark-acclimated for at least 30 min, using DLC-8 Dark Leaf Clips (Walz). After measurement of the minimum fluorescence in the dark-adapted state (F_0), a short, strong pulse of red light (intensity 10; 0.1 s) was applied to measure the maximal fluorescence (F_m). Maximal quantum yield of PSII was calculated using the equation $F_v/F_m = (F_m-F_0)/F_m$ (Genty et al. 1989).

Leaf gas exchange and chlorophyll fluorescence analyses were performed using the equipment provided by the PRAMMICS platform (OSU-EFLUVE UAR 3563).

2.5.4 Pigment contents

Immediately after gas exchange, stem water potential and chlorophyll fluorescence measurements, the respective leaves were used for chlorophyll content and flavonol index determination using a DUALEX device (Force-A; Cerovic et al. 2012). Each value represented the average of five measurements per leaf. Each week, values were averaged for each tree. Dualex indices were converted to $chlorophyll_{a+b}$ contents (in $\mu g\ cm^{-2}$), using the linear correlation found between Dualex indices and

spectrophotometrically determined total chlorophyll concentrations obtained after extraction with acetone 80% (Lichtenthaler, 1987) from 22 plane leaves presenting different physiological states (Dualex index = 0.5222[Chla+Chlb], with R^2 = 0.8953).

2.5.5 Carbon and nitrogen elementary and stable isotope analyses

Leaf sampling for ^{13}C isotopic analyses occurred before (13 May 2022) and at the end of the drought period (16 June 2022). Leaves collected for stem water potential measurements were dried at 60°C for 72h and ground by shaking twice for 30 s at 30 Hz, with five 0.5 mm stainless beads in 50 mL tubes, using a bead grinder (TissueLyser II, Qiagen). The powders were sieved at 200 µm and 0.8-1.2 mg were weighed in tin capsules. The analyses of $\delta^{13}C$ and C/N ratio were carried out at the Alysés-IRD technological platform (Bondy, France). After complete combustion of samples, C and N elementary analyses were performed (Flash HT elemental analyser, Thermofisher) and the isotopic ratio was determined with a mass spectrometer (Delta V Advantage, ThermoFisher). For carbon isotope ratio, the Vienna Pee Dee Belemnite (VPDB) was used as a reference and the results of $\delta^{13}C$ were expressed in the conventional δ notation: $\delta^{13}C = [[(^{13}C/^{12}C)_{sample}-(^{13}C/^{12}C)_{VPDB}] / (^{13}C/^{12}C)]_{VPDB} *1000$. For Nitrogen isotope ratio, the air Nitrogen was used as a reference and the results of $\delta^{15}N$ were expressed in the conventional δ notation: $\delta^{15}N = [[(^{15}N/^{14}N)_{sample}-(^{15}N/^{14}N)_{air}] / (^{15}N/^{14}N)_{air}]*1000$. C and N isotope measurements were conducted at a precision of 0.05‰ and 0.1‰, respectively, and C and N contents at a precision of 0.05%.

2.6 Biochemical and metabolomic analyses

Three mature leaves per tree were sampled from each tree on 13 May 2022 and 17 June 2022, immediately frozen in liquid nitrogen and stored at -80°C until further processing. The frozen material was ground to a fine powder in liquid nitrogen using a mortar and pestles. Powder aliquots from the three leaves collected on the same tree were pooled together prior to biochemical and metabolomic analyses (except for trees 1A and 1B that were not analyzed; n=5 per treatment).

The proline content was measured according to the procedure described by Magné and Larher (1992). Briefly, 50 mg of frozen leaf powder was dissolved in 1 mL sodium citrate buffer (0.2 M, pH 4.6). A 1% ninhydrin solution was added, and the mixture was boiled to form a proline-ninhydrin complex, which was subsequently extracted with toluene and quantified spectrophotometrically at 520 nm (Implen NP80 Nanophotometer®). The Malondialdehyde (MDA) was quantified according to the procedure described by Heath and Packer (1968), using 50 mg of frozen leaf powder and 1.5 mL of extraction solution (0.5% thiobarbituric acid and 20% trichloroacetic acid, in distilled water). After heating the mixture at 95°C for 30 min and a quick cooling on ice, the extract was centrifuged at 12 800x*g* at 4°C for 5 min. After three-fold dilution of the supernatant, the absorbance was measured at

532 nm and at 600 nm, using a nanospectrophotometer (Implen NP80 NanoPhotometer®). The MDA contents were calculated using the MDA molar absorption coefficient (ε) of 155 mmol.cm^{-1}, according to the following formula:

C_{MDA} (nmol g^{-1}_{FW}) = (Δ532nm-600nm*V_{Total}*1000) / (ε.λ*sample mass)

The concentration was expressed per g of leaf dry matter using the water content values (WC) calculated previously (see 2.5.2).

For metabolic profiling, three technical replicates per tree were used, each corresponding to 100 mg of frozen leaf powder. After freeze-drying, polar metabolites were extracted with a mixture of MeOH/Chl/H_2O containing internal standards (100 µM beta-aminobutyric acid and 200 µM adonitol). The MeOH/H_2O fraction was used to analyse amino acids, sugars and organic acids by UPLC-DAD and GC-FID methods by combining derivatization steps and chromatographic elution, following procedures described previously (Dellero et al. 2020; Bianchetti et al. 2021). Metabolite identification was established according to their retention times with respect to chemical derivatized standards. Metabolite quantification was performed using calibration curves of standards and by considering internal standard signals. All metabolite contents were expressed in µmol g^{-1}_{DW}. The raw data are available online (DOI: 10.57745/SWF5U8).

2.7 Statistical analyses

Data were analysed using the R software v4.2.2 (R Core Team 2023) in RStudio 2023.03.0+386 with packages *ggplot2*, *cowplot*, *nlme*, *emmeans*, *car*, *voxel*, *gamm4*, *mscV* and *MuMin* for data representation and statistical modelling. To test for variations between weeks and the impact of drought, a linear mixed effect model (*nlme::lme*) was calculated (using the formula: y ~ treatment * week) with treatment (control or drought) and week (17 to 24) as fixed effects. The tree individual was included in the model as a random effect (~1|tree). Normality and homoscedasticity of the residuals were checked by visual inspection. Variables failing to meet these assumptions were mathematically transformed (log or reflect-log transformed) and the residuals were checked again to confirm normality and homoscedasticity of their distribution. Mixed effect model was analysed through a type II ANOVA (*car::Anova*). Estimated marginal means were computed using *emmeans::emmeans* before doing a post-hoc test with Tukey correction using the *emmeans::contrast* function. To test for daily variations, a generalized additive mixed model (*gamm4::gamm4*) was calculated (using the formula: y ~ treatment + s(date), with treatment (control or drought) as a fixed effect and date (time of the day) as a smooth term. The tree individual was included in the model as a random effect (~1|tree). Mixed effect model was analysed through a type II ANOVA (*car::Anova*) and 95% Confidence Interval was extracted using *voxel::plotGAMM* function. For metabolomic data, correlation between metabolites was analysed

using Spearman's rank sum non-parametric test. Differences between groups were analysed using a non-parametric Wilcoxon Mann-Whitney test and p-values were adjusted using Holm's method. Metabolites significantly impacted were analysed using Principal Component Analysis (PCA) (*FactoMineR::PCA*). For these metabolites, Z-score were calculated for heatmap representation. All the data were plotted with *ggplot2, factorextra, ComplexHeatmap, corrplot* or *cowplot* packages. Data in text and tables are given as mean ± Standard Error of the Mean (SEM).

3 Results

3.1 Meteorological parameters, soil and tree water status

Meteorological parameters were recorded from 9 May 2022 to 16 June 2022 (weeks 19-25), a period characterized by low precipitations (69 mm) (Fig. 1a). During this period, weekly mean air temperatures (T_{air}) were comprised between 15.26 ± 0.11 °C and 23.54 ± 0.18 °C, with the week 21 being the coolest and the week 24 the warmest. Weekly average Vapor Pressure Deficit (VPD) was between 0.7 ± 0.01 and 1.81 ± 0.03, with weeks 21 and 24 being also the most humid and driest, atmospherically. The study period was characterized by a strong heterogeneity in PAR. Weekly means ranged between 516.8 ± 16.37 and 741.31 ± 20.55 µmol m^{-2} s^{-1} for the cloudiest and sunniest weeks (weeks 21 and 24), respectively (Fig. 1b).

The drought experiment was carried out over weeks 20-25, between 18 May 2022 and 16 June 2022. While watering was completely withheld from droughted trees, control trees were watered with an average of 5.5 L day^{-1} (Fig. 1c). Extractable soil water content (eSWC) was rather homogeneous (p-value = 0.64, ANOVA) along the vertical profiles of the containers, in both control and droughted trees (Fig. S2). In control trees, eSWC was stable at around 45%, with a temporary decrease to 35% at week 23 (Fig. 2a). In droughted trees, the initial eSWC was significantly higher than that of the control trees. In response to water withholding, eSWC declined following a biphasic pattern with an initial sharp drop from 50% to 35% eSWC reached at the end of week 22 [at this time-point, the eSWC of droughted trees was significantly lower than that of control trees (p-value < 0.01, Tukey HSD test)], followed by a slower decrease from 35% to 30% over weeks 23 and 24 [at this last time-point, eSWC remained significantly lower than that of control trees (p-value < 0.01, Tukey HSD test)].

Control and droughted trees had equivalent stem water potential (Ψ_{stem} ~ -1.0 MPa) from week 19 to week 21 (Fig. 2b). As of week 22 (*i.e.* two weeks into the drought treatment), the Ψ_{stem} of the droughted trees remained significantly lower than that of the controls (p-value < 0.001, Tukey HSD test). In droughted trees, the small drop in Ψ_{stem} from ~ -1.0 MPa to -1.5 MPa that occurred over weeks 19-22 corresponded to the phase of considerable loss in eSWC. The further sharp decline in Ψ_{stem} to -2.3 MPa

corresponded to a minor loss in eSWC. It should be noted that the Ψ_{stem} of control trees temporarily dropped to -1.4 MPa between weeks 23 and 24 (Fig. 2b).

Relative water content (RWC) remained unchanged at > 80% over most of the experiment, regardless of the treatment (p-value = 0.38, two-way ANOVA) (Fig. 2c). However, between weeks 23 and 24 (*i.e.* four weeks into the drought treatment), the RWC of the droughted trees was significantly lower than that of the control trees (-15%; p-value < 0.05, Tukey HSD test).

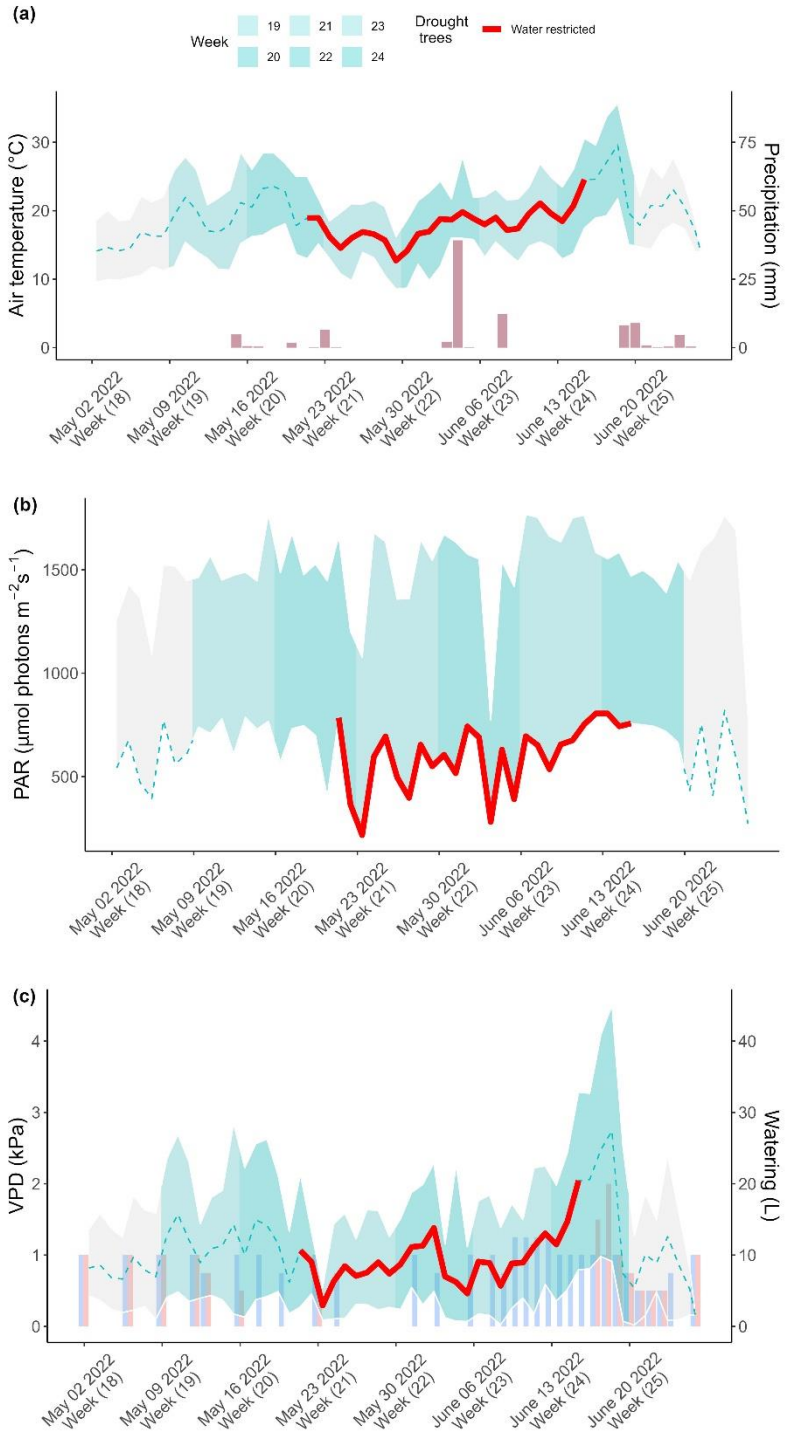

Fig. 1: **Meteorological parameters from May 2022 to June 2022.**

(**a**) Air temperature (T_{air}) and precipitations, (**b**) Photosynthetic Active Radiation (PAR) and (**c**) Water Vapor Pressure Deficit (VPD) and watering. In (a and c), line and interval represent the daily median and range (minimal and maximal) values for T_{air} and VPD, respectively. In (b), line and interval represent the daily median and range (median and maximal) values for PAR > 50 $\mu mol_{photons}$ m^{-2} s^{-1}, respectively. Weekly periods of measurements are shown in light and darker blue, corresponding to uneven and even week numbers, respectively. Dashed lines indicate periods of homogenous watering regime, while red lines indicate the period of water withholding applied to droughted trees. In (a and c), bars indicate the daily precipitations (mm) and watering (L per pot), respectively. In (c), blue and red bars correspond to the water applied to control and droughted trees, respectively.

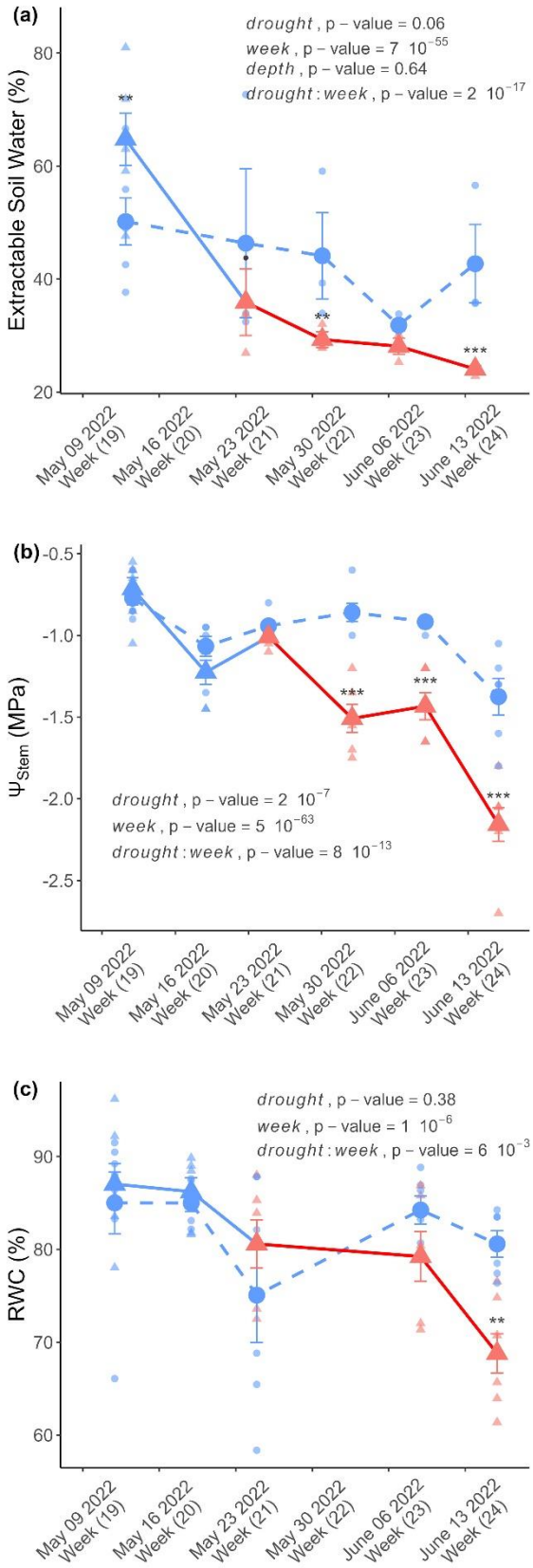

Fig. 2: Soil and plane tree water status over the experiment.

(**a**) Extractable soil water content. (**b**) Stem water potential and (**c**) Leaf relative water content. Triangles (▲) with solid line and circles (●) with dashed line represent droughted trees and control trees, respectively. For (a), the values are the means of the measurements at the four depths (see Fig. S2 for values at specific depth). Small symbols represent individual trees, while larger ones represent the weekly mean value (n=6), with vertical error bars representing the S.E.M. The symbol color corresponds to the watering, with blue and red indicating trees without or with water withholding, respectively. Significance of variations between weeks, in response to drought or the interaction of both factors are presented on the figure (linear mixed model followed by a type II ANOVA). Asterisks indicates significance differences between drought and control trees in the week (Tukey HSD post-hoc test, *** p-value < 0.001, ** p-value < 0.01, * p-value < 0.05, ● p-value < 0.1).

3.2 Genetic analysis

The genetic profiling of the young plane trees was conducted using 10 microsatellite loci (Table S2) and seven reference trees (Table S1). Results confirmed that all the 14 young trees were *Platanus* × *hispanica* (Table S3) and that they were clones likely exhibiting somatic variations (Table S3). It is noteworthy that an adult (more than 70 years old) plane tree planted next to the experimental site had the same genetic profile as the young trees (Table S3).

3.3 Canopy development

The canopy development was analysed on selected branches throughout the experiment. By mid-April 2022 (week 17), the canopies of the containerized young plane trees had their maximum number of leaves (Fig. 3a), while the maximum leaf area was only reached in week 22 (Fig. S4a). Over weeks 17-21, the overall leaf numbers in the canopies decreased very slightly. Compared to the controls, the to-be-droughted trees showed some fluctuation in their leaf number and, at week 20, their relative leaf number was higher than that of the controls due to a significantly larger batch of emerging leaves (Fig. 3a and Table S4). At the final stage of the drought treatment, between weeks 22-24, the droughted trees significantly lost (p-value < 0.01, Tukey HSD test) more leaves than the controls (Fig. 3a, 50% and 8%, respectively), leading to a decrease in leaf area (Fig. S4) and is consistent with visual observations (Fig. 3b).

Individual leaf surface was estimated using an allometric relation (Fig. S3). At the branch level, the total leaf surface showed a significant linear correlation with the number of leaves ($R^2 > 0.86$; Fig. S4), the slope corresponding to the mean leaf surface (29.80 cm^2). The drought treatment induced a higher mean leaf surface, suggesting a preferential loss of smaller leaves.

Over the measurement period, leaf chlorophyll contents exhibited a “bell-shaped” pattern with equivalent starting and final levels and a maximum plateau between weeks 21-22 (Fig. 3c). In contrast, leaf flavonol contents continuously increased throughout the period (Fig. 3d). The drought treatment had no significant effect on either chlorophyll or flavonol contents (p-value > 0.05). However, other leaf features were impacted by the drought treatment: the droughted trees had significantly more leaves with necrosis and yellowing than the controls between weeks 22-24 (Table S4). Before the application of the treatment, the to-be-droughted trees suffered from more severe attacks by the *Platanus* lace bug at week 19 (Table S4).

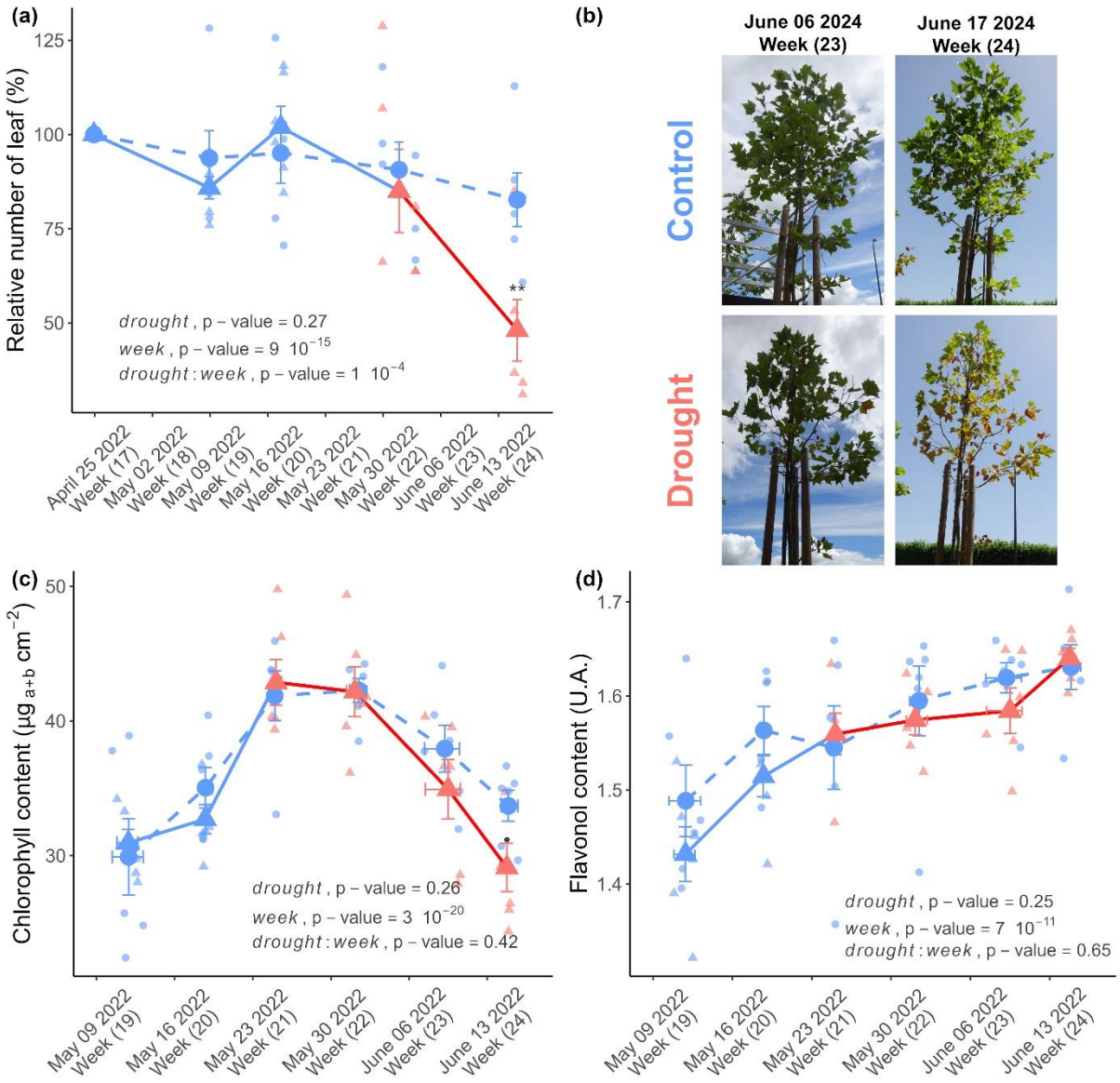

Fig. 3: Plane tree canopy development and evolution of biochemical indicators over the experiment.

(**a**) Relative leaf number, (**b**) representative photographs of the state of the canopy during the drought, (**c**) total chlorophyll and (**d**) flavonol contents. Relative leaf number (a) was expressed relative to the initial leaf number (100 %) determined on week 17. Photograph (b) were taken on June 6th (left column) and 17th (right column) 2024, 16 and 27 days after the water withholding started for droughted trees (bottom row). Triangles (▲) with solid line and circles (●) with dashed line represent droughted trees and control trees, respectively. Small symbols represent individual trees, while larger ones represent the weekly mean value (n=6), with vertical error bars representing the S.E.M. The symbol color corresponds to the watering, with blue and red indicating trees without or with water withholding, respectively. For (a), (c) and (d), the significance of variations between weeks, in response to drought or the interaction of both factors, are presented on the figure (linear mixed model followed by a type II ANOVA). Asterisks indicates significance differences between drought and control trees in the week (Tukey HSD post-hoc test, *** p-value < 0.001, ** p-value < 0.01, * p-value < 0.05, ● p-value < 0.1).

3.4 Photosynthetic leaf traits

In control trees, leaf photosynthetic parameters varied little during the season except for a brief decrease at week 21 (Fig. 4). During the experiment, light-saturated net CO_2 assimilation (A_{sat}) values ranged from 8.4 to 11.2 µmol m^{-2} s^{-1} (Fig. 4a), stomatal conductance (G_s) from 81 to 135 mmol m^{-2} s^{-1} (Fig. 4b), internal CO_2 concentration (Ci) from 192 to 253 µmol $mmol^{-1}$ (Fig. 4c) and maximal quantum yield of PSII (F_v/F_m) from 0.76 to 0.79 (Fig. 4d). The photosynthetic parameters A_{sat}, Ci and G_s of the droughted trees were equivalent between drought and control treatments until week 21, despite the restriction of water supply started at week 20. Between weeks 21 and 22, A_{sat}, G_s and C_i plunged significantly (p-value < 0.01, Tukey HSD test), with 70%, 67% and 32% reductions, respectively. On the other hand, the maximum yield of PSII remained unaffected (Fig. 4d). Over weeks 23-24, in the droughted trees, both A_{sat} and G_s remained low (1.7 µmol.m^{-2}.s^{-1} and 16 mmol.m^{-2}.s^{-1}, respectively), C_i rose back to control values and F_v/F_m declined below control values (3% and 5% reductions, in week 23 and 24, respectively). Daily maximum G_s values measured in ambient conditions were drastically reduced (-50%) after week 20 in all trees. Stomata of droughted trees remained fully closed during weeks 22 and 23 (Fig. S5).

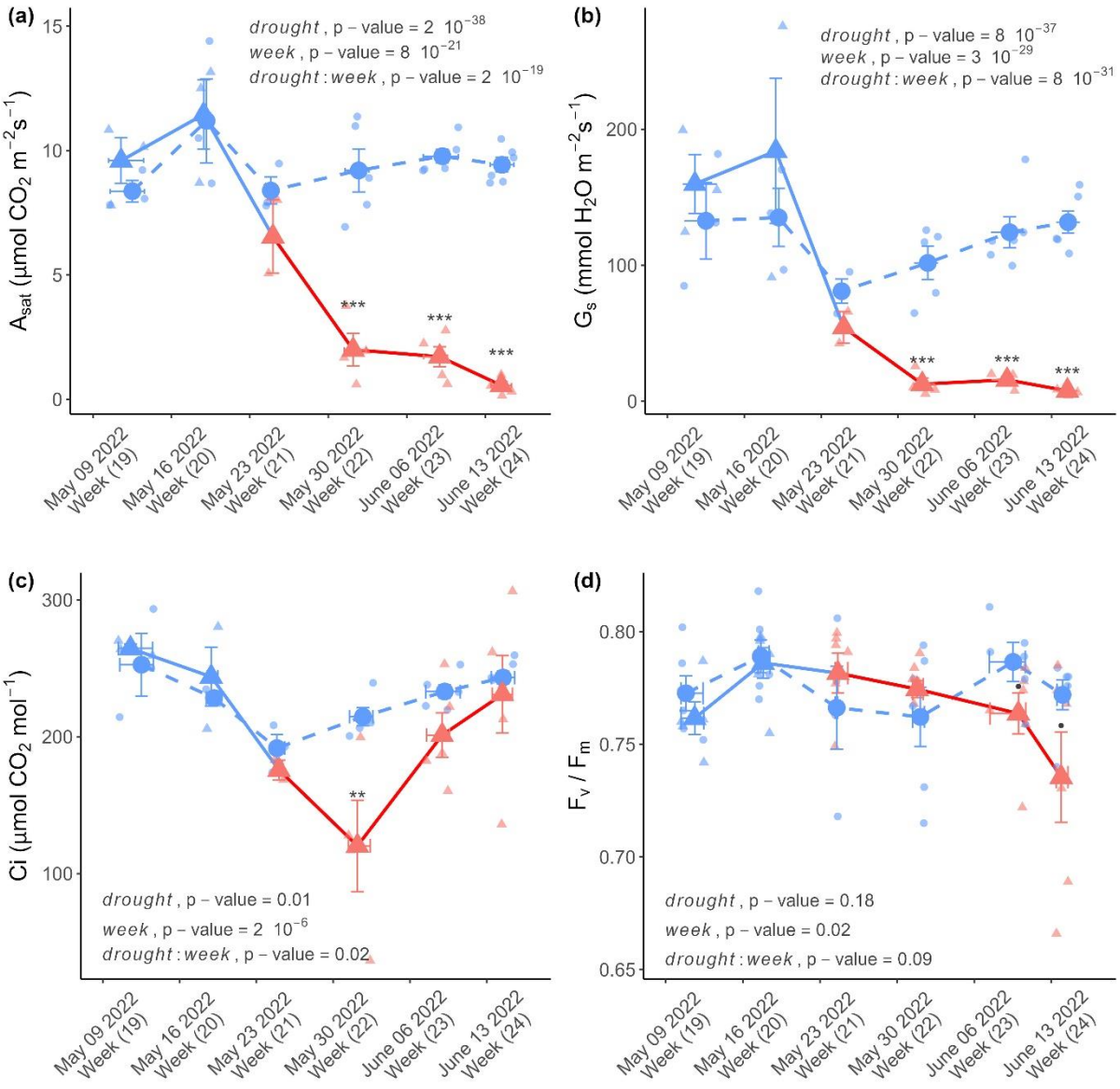

Fig. 4: Leaf gas exchange and chlorophyll fluorescence over the season.

(**a**) Light- saturated net CO_2 assimilation rate (A_{sat}), (**b**) stomatal conductance to water vapor (G_s), (**c**) lLeaf internal CO_2 concentration (Ci) and (**d**) maximal quantum yield of PSII photochemistry (F_v/F_m). Triangles (▲) with solid line and circles (●) with dashed line represent droughted trees and control trees, respectively. Small symbols represent individual trees, while larger ones represent the weekly mean value (n=3 to 6), with vertical error bars representing the S.E.M. The symbol color corresponds to the watering, with blue and red indicating trees without or with water withholding, respectively. Significance of variations between weeks, in response to drought or the interaction of both factors, are presented on the figure (linear mixed model followed by a type II ANOVA). Asterisks indicates significance differences between drought and control trees in the week (Tukey HSD post-hoc test, *** p-value < 0.001, ** p-value < 0.01, * p-value < 0.05, ● p-value < 0.1).

3.5 Leaf carbon and nitrogen composition

Leaf carbon content significantly increased over the experiment (May-June 2022) in both control (+5%) and droughted (+3%) trees and it was not impacted by drought (Table 1). Nitrogen content followed an opposite pattern, with a significant decrease during the season. Prior to the drought treatment, the

leaves of the trees that were droughted later contained 25% more nitrogen than control leaves. At the end of the drought treatment, droughted trees showed a more pronounced decrease in leaf nitrogen content (-35%) than control ones (-25%). Consequently, the C:N ratio significantly increased between May and June, with no significant impact of the drought treatment. Finally, stable isotope compositions in $\delta^{13}C$ and $\delta^{15}N$ were equivalent before the treatment and drought significantly reduced the ^{13}C discrimination (Table 1).

Table 1: C and N composition, proline and MDA contents of leaves. Leaf elemental and stable isotope analyses were performed twice during the experiment on 13 May 2022 (before water withholding) and on 16 June 2022 (29 days after the beginning of water restriction). Analyses were performed on the leaves used for Ψ_{stem} determination and values represent the mean ± SEM (n=6). Different letters indicate significant differences between groups (p-value < 0.05, linear mixed model followed by Tukey HSD test).

		Elemental			Stable isotope		Biochemistry	
Date	Treatment	**C (g kg^{-1}_{DW})**	**N (g kg^{-1}_{DW})**	**C:N ratio**	**$\delta^{13}C$ (‰$_{VPDB}$)**	**$\delta^{15}N$ (‰$_{N2}$)**	**Proline (nmol g_{DW}^{-1})**	**MDA (µmol g_{DW}^{-1})**
13 May 2022 *Week (19)*	Control	495.9 ± 0.8 ^{a}	23.2 ± 0.9 ^{b}	21.5 ± 1 ^{a}	-27.5 ± 0.1 ^{a}	2.3 ± 0.2 ^{a}	763 ± 93 ^{ab}	1.6 ± 0.1 ^{a}
	Drought*	497.9 ± 3.6 ^{a}	29.1 ± 1 ^{c}	17.2 ± 0.6 ^{a}	-26.2 ± 0.3 ^{ab}	3.1 ± 0.3 ^{a}	952 ± 156 ^{b}	1.4 ± 0.2 ^{a}
16 June 2022 *Week (24)*	Control	518 ± 3.3 ^{b}	17.4 ± 1.4 ^{a}	30.7 ± 2.2 ^{b}	-27.3 ± 0.3 ^{a}	2.6 ± 0.3 ^{a}	329 ± 76 ^{a}	1.7 ± 0.1 ^{a}
	Drought**	514 ± 0.6 ^{b}	19.1 ± 0.4 ^{ab}	27.2 ± 0.6 ^{b}	-25.9 ± 0.4 ^{b}	3.1 ± 0.3 ^{a}	1225 ±178 ^{b}	1.5 ± 0.1 ^{a}

* Before water withholding (WW) ; ** 29 days after WW started

3.6 Biochemical and metabolome analyses

Leaf MDA contents remained unchanged in response to the drought treatment (Table 1). Leaf proline contents, on the other hand, showed a 3.7-fold increase in the leaves of the droughted trees (Table 1). Targeted metabolic profiling focused on amino acids, sugars, polyols and organic acids was conducted on leaves harvested from each tree before and after the drought treatment. The results revealed high variability for many amino acids and sugars within the same tree (technical replicates) and between trees under the same conditions (biological replicates). The most abundant carbon metabolites detected in our analysis were fructose, glucose, sucrose, malate and quinate, ranging from 10 to 80 µmol g^{-1}DW (Figs 5 and S6). In contrast, amino acids' concentrations were lower than for carbohydrates, with a maximum of 10 µmol g^{-1}DW for glutamine. Nevertheless, a statistical analysis of the results

unveiled nine differentially accumulated metabolites in response to the season, primarily sugars or organic acids classes, with serine as the only amino acid (Fig. S6).

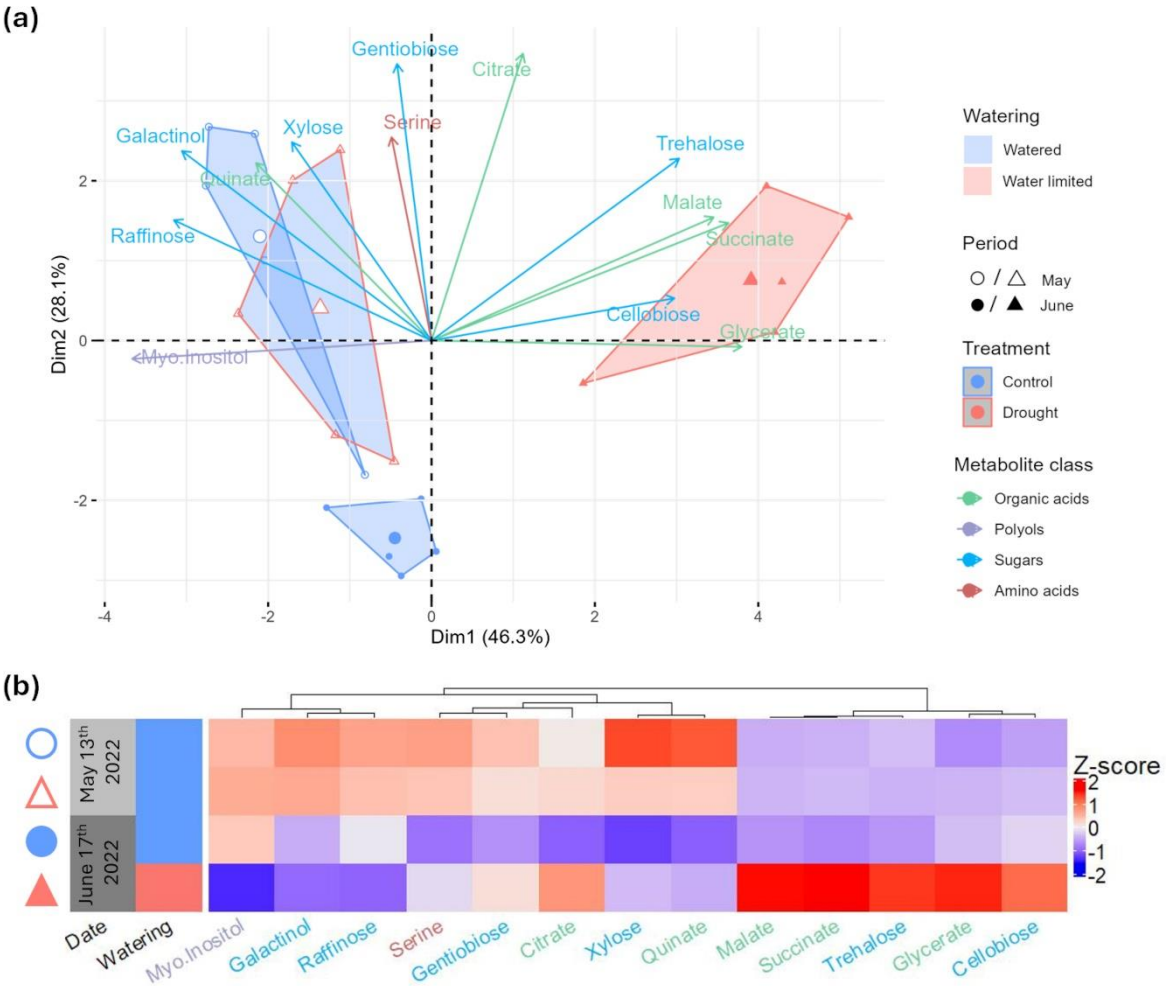

Fig. 5: Targeted metabolomic profiling. (**a**) Principal component analysis of the metabolites responding to drought and/or seasonality (for details see Fig S6 and S7) and (**b**) heatmap of the metabolite Z-score value. For PCA (a), the first and second dimension explains 46.3%, and 28.1%, respectively. Arrows shows the contribution of the metabolites and colours indicates the class. Triangles (▲ or△) connected by red convex hull and circles (● or ○) connected by blue convex hull represent droughted trees and control trees, respectively. Empty and filled symbols corresponds to the samples collected May 13th and June 17th, respectively. Filling colour of convex hull corresponds to the watering, with blue and red indicating trees without or with water withholding, respectively. Heatmap (b), shows the z-score value of each metabolite. Red and blue denote high and low Z-score values of metabolites. Metabolites were clustered according to euclidian distances.

PCA analysis shows distinct patterns: the two principal dimensions collectively explained 74.4% of the variance, with PC1 contributing 46.3% and PC2 28.1% (Figs 5a and S7). Interestingly, TCA compounds such as succinate and malate, as well as glycerate, trehalose, cellobiose, raffinose, galactinol, xylose

and myo-inositol exhibited significant inter-correlations (Fig S8). The first dimension effectively delineated the impact of drought treatment. In contrast, citrate, serine and gentiobiose highly contributed to the second dimension and seemed associated with seasonal variations (Figs 5a and S7). While cellobiose and glycerate were more abundant in June than in May, malate, quinate, succinate, galactinol, trehalose and xylose contents decreased with time (Figs 5 and S6). Thus, the major seasonal variations were reductions in quinate, xylose and galactinol contents (Fig. S6). Moreover, the drought treatment altered the abundances of 12 metabolites (with no amino acid included): cellobiose, citrate, gentiobiose, glycerate, malate, quinate, succinate, trehalose and xylose abundances increased, while galactinol, myoinositol, raffinose contents were reduced (Fig. S6). The main changes in response to drought were increases in malate (9.7-fold), trehalose (3.7-fold), glycerate (2.1-fold), xylose (absent in control), quinate (1.5-fold) and a decrease in myo-inositol (2-fold) (Fig. S6). Regarding proline, metabolomic and spectrophotometric analyses both indicated an increase in response to drought but it was not statistically significant for metabolomics (Table 1 and Fig S6).

4 Discussion

4.1 Experimental setup in urban conditions

Our experimental setup was designed to study plane tree physiology in urban conditions in response to a severe drought. The genetic analysis showed high similarity between young trees, confirming their production by vegetative multiplication through cuttings (Morton and Gruszka 2008). The setup consisted of ready-to-plant plane trees growing in black containers situated 15 cm above black asphalt and aligned in an East-West orientation with no-overlapping canopies. These conditions likely impacted the trees' summer growth conditions, notably through high exposure to solar radiation and T_{air} (Rinaldi et al. 2019; Sanusi and Livesley 2020) due to the additional energy from the asphalt's high surface temperatures amplified by the black containers (Kjelgren and Montague 1998). An original feature of this setup was the custom-made rain exclusion systems that proved highly effective since no significant increase in eSWC was observed even after heavy rainfall. Thus, the water supply to the plane trees was efficiently controlled: despite episodes of high T_{air} and atmospheric drought during the May-June 2022 study, fluctuations in eSWC to well-watered trees were small because eSWC depletion was regularly compensated for (Figs 1 and 2). Even the temporary decline in eSWC during week 23, observed as a result of strong evapotranspiration stimulated by a severe increase in air temperature (and thus in VPD), did not compromise the stock of readily available water (eSWC > 30 %; Rahman et al. 2023) or impact the physiology of the trees: their stomatal conductance, stem potential and RWC remained unaffected (Figs 2 and 4b). This episode, however, illustrates the challenge of maintaining a constant

water supply to potted plants in urban setups over several weeks. It should be noted that the vertical profile of the soil water content in the pots (Fig. S2) suggested an homogenous soil colonization by roots (Monshausen and Gilroy 2009; Cassab et al. 2013), which was confirmed by visual inspection of root systems after uprooting (data not shown). Thus, it was not surprising to observe C assimilation and stomatal conductance values (Figs 5 and S5) equivalent to those obtained on younger also well-watered *P.* × *hispanica* trees (around 12 µmol CO_2 m^{-2} s^{-1} and 150 mmol H_2O m^{-2} s^{-1} ; Tattini et al. 2015). Gillner et al. (2015) measured gas exchange of urban *P.* × *hispanica* adults that were lower than our measurements (around 5 µmol CO_2 m^{-2} s^{-1} and 30-50 mmol H_2O m^{-2} s^{-1}), suggesting that our plane trees were well adapted to their pots.

4.2 Seasonality of plane tree physiology

Several elements indicated that well-watered trees experienced changes inherent to seasonality. Leaf chlorophyll contents increased at the beginning of the season concomitantly with leaf development (Figs 3 and S4), as expected (Bisba et al. 1997; Rahman et al. 2023). However, they declined unexpectedly long before the end of the summer, suggesting early leaf senescence likely triggered by biotic factors and heat stress (Ristic et al. 2007; Gillner et al. 2017). The plane trees were indeed infested by the *Platanus* lace bug, *Corythucha ciliata* (Table 1), an insect causing leaf-feeding damage that progresses into chlorotic or bronzed foliage and premature loss of leaves (Tubby and Webber 2010; Ju et al. 2017). This decrease in leaf chlorophyll content associated with a decrease in N content had no consequence on A_{sat} and F_v/F_m, as is usually observed in herbaceous species (Dellero et al. 2021). Other leaf pigments, like flavonols, gradually increased during the season (Fig. 4), probably in response to changes in meteorological parameters (increase in T_{air} and PAR) and abiotic pressure. *P.* × *hispanica* leaves are known to be rich in phenolic compounds, with flavonol quercetin-3-O galactoside as the most abundant (Ribeiro et al. 2022). Along with early chlorophyll loss, increasing leaf flavonol contents was an indication that well-watered trees were in fact affected by the combination of biotic and abiotic factors since flavonols accumulation is linked to leaf acclimation to light (Xu et al. 2014) and stress (Winkel-Shirley 2002; Yu et al. 2021; Laoué et al. 2022).

To characterize the biochemical changes over the season, a metabolomic analysis was performed. Results indicated that very few leaf metabolites showed significant seasonal variation (Figs 5 and S6), probably as a consequence of a large variability between biological replicates. Nevertheless, an important decrease in quinate was observed between May and June for control trees. Quinate is a precursor of chlorogenic acids (CGAs) (Gritsunov et al. 2018) that represent 19% of the total phenolics identified in *P.* × *hispanica* (Ribeiro et al. 2022). CGAs serve as antioxidants in response to UV radiation, as antifungal agents and help deter herbivory (Carrington et al. 2018). The high biotic pressure observed at the beginning of the season (see lace bugs, Table S4) could explain the plummeting in

quinate, potentially linked to an increase in CGAs. Xylose, the main hemicellulose monosaccharide in plane leaves, as in other broadleaved trees (Schädel et al. 2010), decreased between May and June. This variation may be linked to the seasonal regulation of leaf and stem vascular tissue construction (Prislan et al. 2013; Montwé et al. 2019; Macieira et al. 2021). Overall, quinate and xylose levels were important indicators of seasonal regulation of plane tree biology, showing robust repeatability and a strong correlation (Fig. S8) in realistic urban growth conditions.

4.3 Drought impact on tree physiology

Water restriction was imposed by total water withholding during five consecutive weeks. Within the first two weeks, the eSWC sharply declined to approximately 35%, just above the critical 30% limit corresponding to the readily available water. This coincided with a drop in stem water potential to -1.5 MPa, and with the stomatal limitation (SL) of A_{sat}, as shown by C_i decline. Since leaf RWC and chlorophyll contents remained unaffected compared to the control trees, the decrease in stem water potential did not result from leaf turgor loss or leaf structural damage. Most likely, it could be induced by ABA accumulation and osmotic adjustment as part of a drought avoidance strategy (Arndt et al. 2008; Turner 2018). Previous studies demonstrated that drought avoidance, leading to isohydric behaviour, predominated in *P.* × *hispanica* submitted to water deficit (Tattini et al. 2015; Caplan et al. 2019; Franceschi et al. 2023), even though others described the species as anisohydric (Hirsch et al. 2023; Rahman et al. 2023).

The second stage of the drought treatment lasted three weeks. It corresponded to further losses in eSWC (from 35% to 25%) and the development of actual drought stress in the trees, including a further decrease in stem water potential to -2.2 MPa, in leaf RWC and chlorophyll contents, as compared to the controls. Irreversible damage to the photosynthetic apparatus corresponding to non-stomatal limitation (NSL) of photosynthesis was suggested by a rise in C_i, while G_s remained low, and by a reduction in the maximal quantum yield of PSII (F_v/F_m). Similar responses were previously observed on young plane trees after 10-11 and 15-16 days of stress, leading to SL and NSL of photosynthesis, respectively (Tattini et al. 2015).

All canopies were fully developed by late April 2022 since very few leaves emerged after (Table S4). During the first phase of the drought treatment that corresponded to moderate drought stress (Ψ_{stem} > -1.5 MPa), the plane tree developed water-saving strategy at the cellular level. Continuing drought induced severe defoliation at the very end of the treatment when Ψ_{stem} < -2MPa. This defoliation is a well-described strategy to reduce evaporative demand at the tree level in *Platanus* (Sanusi and Livesley 2020; Marchin et al. 2022).

Maintenance of water content and protection of photosynthetic apparatus in response to mild drought came with biochemical changes. To comprehensively investigate these changes, we performed a leaf-targeted metabolome that showed an increase in total metabolite contents (2467 µmol g^{-1}DW in droughted trees *vs* 1859 µmol g^{-1}DW in control trees). This suggests that reduction in growth (C demand) prevailed over photosynthesis limitation (C supply), as observed in several species (Bogeat-Triboulot et al. 2007; Fàbregas and Fernie 2019) and that active metabolome reprogramming took place (Xu and Fu 2022). Large amounts of tricarboxylic acid cycle (TCA) intermediates, such as malate, succinate and citrate (20, 2 and 2 µmol g^{-1} DW, respectively; Figs 5 and S6), accumulated in response to the drought treatment, as previously shown in herbaceous species such as Arabidopsis and tomato (Semel et al. 2007; Pires et al. 2016). TCA cycle reprogramming in response to drought is highly complex and understanding the underlying mechanisms requires further focused research (Fàbregas and Fernie 2019). Nevertheless, massive accumulation of malate during drought was already observed in *Fraxinus excelsior*, where it was considered as the main osmoticum (Guicherd et al. 1997). Here, the accumulation of malate likely contributes to the osmotically-driven decline in stem water potential during the water-saving phase of the drought response.

Most of the proteinogenic amino acids detected in plane leaves, beside proline, were not significantly modified by drought. However, proline accumulated to final contents that were relatively low (around 1 µmol.g^{-1} DW) compared to those found in droughted herbaceous plants (40 µmol.g^{-1} DW for Arabidopsis, 300-500 µmol.g^{-1} DW for *Brassica napus*), where it increases the cellular osmolarity during water limitation (Verslues and Sharma 2010; Albert et al. 2012). In *Platanus orientalis* leaves, previous measurements have already shown low proline levels (5 – 13 µmol.g^{-1} DW; Cui et al. 2022; Mukhamedova et al. 2022). This suggests that, in *Platanus*, proline accumulation may not contribute significantly to cellular osmotic adjustment and could therefore serve as a redox regulator within the cell (Zheng et al. 2023). The correlation analysis of metabolome (Fig S8) highlighted several groups of correlations. Unexpectedly, a clear group of amino acids correlated together, suggesting a common regulation pattern. This was confirmed by the fact that the total individual amino acid contents increased in response to drought (393 µmol g^{-1} DW in droughted trees *vs* 232 µmol g^{-1} DW in control trees). This global trend could result from several processes related to growth arrest, senescence or metabolome reprogramming. Like proline, leaf MDA did not appear as a robust marker of water stress in this experiment, probably due to high levels found in control trees. Indeed, the MDA contents observed here were 3 to 20-fold higher than those measured in adult *P.* × *hispanica*, *P. orientalis*, pine, olive tree or oaks subjected to urban or water stresses (Sofo et al. 2004; Tattini et al. 2015; Zhang et al. 2021; Cui et al. 2022; Xiong et al. 2022). Moreover, we have noticed high discrepancies in reported MDA leaf contents in the literature (around 5 µmol.g^{-1} DW in control olive trees (Parri et al. 2023), 10-25

µmol.g^{-1} DW in *P. orientalis* growing in urban conditions (Mukhamedova et al. 2022), a fact that led us to question the pertinence of this compound as a water stress marker in plane trees. Other major antioxidant compounds (flavonols) were not affected by the drought treatment but increased regularly during the season in both control and droughted trees, suggesting that antioxidant potential was progressively required in response to the multifactorial and stressful environments of cities.

Although Raffinose Family of Oligosaccharides (RFO) metabolism (myo-inositol, galactinol, raffinose) is known for its role in desiccation tolerance across diverse organisms (Sengupta et al. 2015), our results did not show such function in plane tree, as these compounds were poorly abundant in all conditions and even decreased during drought. Conversely, trehalose, a non-reducing disaccharide, significantly accumulated (3-fold) during drought and could potentially participate in the osmotic adjustment of the water-saving response of the plane trees. Furthermore, threalose-6P is considered a key regulator of carbon sensing and partitioning, activated in response to drought (Carraro and Di Iorio 2022), notably to stimulate ABA-triggered stomatal closure in wheat, cotton and *Citrus* (Lunn et al. 2014; Santana-Vieira et al. 2016). Although trehalose metabolism has been poorly documented in woody plants to date, its regulation is considered as a target to improve drought tolerance (Carraro and Di Iorio 2022).

The slight increase in leaf C content during the experiment probably resulted from changes in leaf structure, like cell wall expansion and cuticle thickening, in accordance with leaf xylose depletion. Leaf C content was not significantly impacted by drought, but the slight enrichment in ^{13}C stable isotope confirmed that drought induced a limitation in G_s in droughted trees (Farquhar et al. 1982, 1989). The difference in $\delta^{13}C$ values between droughted and control leaves was equivalent to that observed after drought in urban *P.* × *hispanica* trees (Hirsch et al. 2023). Furthermore, over a five-week period, the leaf N content diminished in both control and droughted trees, with no significant impact of drought.

5 Conclusion

This study characterizes *P.* × *hispanica* as a drought-resistant tree capable of water-loss avoidance strategy, well adapted to urban stress, as described by green space managers of Paris. Several elements confirmed its isohydric strategy that limited eSWC consumption: malate and trehalose accumulation in leaf tissues, likely related to osmotic adjustment, and stomatal limitation of photosynthesis as long as the drought was moderate. Then, when the drought became severe (eSWC <30%), the photosynthetic apparatus was altered and, below the threshold of 25% eSWC, massive defoliation occurred. This defoliation affected the shading potential of the canopy for a short time because rapid re-growth of leaves was possible from the axillary buds exposed after leaf fall. This additional feature characterizes the overall high resilience of plane trees to urban environments. In the context of climatic change in

cities, it would be interesting to analyse the post defoliation events and the impact of successive drought cycles on stored carbohydrates, and the consequences of this strategy on the growth and survival of *P.* × *hispanica* trees in the long term.

Authorship contribution

The experiment was conceptualized by L.L., S.P., J.-F. C., A.R., J.L. and R.P.-F.; A.C., P.N., L.B., L.L., S.P., V.L., J.-F. C., Y.D., A.R., J.L. and R.P.-F performed the experiments; A.C. wrote the original draft and L.L., S.P., Y.D., A.S., A.R., J.L. and R.P.-F. reviewed and edited the manuscript; the students were supervised by A.S., S.P., J.L. and R.P.-F. ; R.P.-F. did the data curation and visualization, and the formal analysis; the project administration was done by L.L. and J.L.; J.L. obtained the funding.

Acknowledgements

The authors wish to thank Stéphane Kerbrat from Genomics platform at Institut Mondor de Recherche Biomédicale, Université Paris-Est Créteil - INSERM U955 (https://imrb.inserm.fr/plateformes/) for sequencing microsatellites and Magloire Mandeng-Yogo from Alysés plateform, IRD Bondy (https://www.ird.fr/la-plateforme-alyses) for isotope analysis. The authors acknowledge Roseline Grouard and Frédéric Achille for access to reference trees in Jardin des Plantes, MNHN, Paris and in Arboretum de Chèvreloup, Versailles. P2M2 (Metabolic Profiling & Metabolomics Platform, Le Rheu, France, https://p2m2.hub.inrae.fr/) and its staff members, especially Solenne Berardocco and Nathalie Marnet, are gratefully acknowledged for carrying out metabolite quantification.

The authors also acknowledge Stéphane Breyne (UPEC) for his technical help in designing & building the total rainfall exclusion systems, the PRAMMICS Platform OSU-EFLUVE UMS 3563 for access to equipment, the IUT Créteil-Vitry (UPEC) for the provision of the experimental site, the “Ville de Paris” tree nursery for providing the plane trees and the services from the “Direction des Espaces Verts et de l’Environnement” and “Direction de la Transition Ecologique et du Climat”, particularly Mathilde Renard and Olivier Chrétien, for their interactions with the researchers. The authors are grateful for Quentin Robert for his implication during his internship.

Data availability statement

The meteorological data of this study are available in the open repository Zenodo DOI: 10.5281/zenodo.12742190. The raw metabolomics data are available online in Recherche Data gouv repository (DOI: 10.57745/SWF5U8).

References

Agliassa C, Mannino G, Molino D, Cavalletto S, Contartese V, Bertea CM, Secchi F (2021) A new protein hydrolysate-based biostimulant applied by fertigation promotes relief from drought stress in *Capsicum annuum* L. Plant Physiol Biochem 166: 1076–1086

Albert B, Le Cahérec F, Niogret M-F, Faes P, Avice J-C, Leport L, Bouchereau A (2012) Nitrogen availability impacts oilseed rape (*Brassica napus* L.) plant water status and proline production efficiency under water-limited conditions. Planta 236: 659–676

Arndt SK, Livesley SJ, Merchant A, Bleby TM, Grierson PF (2008) Quercitol and osmotic adaptation of field-grown *Eucalyptus* under seasonal drought stress. Plant Cell Environ 31: 915–924

Barradas VL, Esperon-Rodriguez M (2021) Ecophysiological vulnerability to climate change in Mexico City's urban forest. Front Ecol Evol 9:732250.

Barrs H, Weatherley P (1962) A Re-Examination of the Relative Turgidity Technique for Estimating Water Deficits in Leaves. Aust Jnl Of Bio Sci 15: 413

Besnard G, Tagmount A, Baradat P, Vigouroux A, Berville A (2022) Molecular approach of genetic affinities between wild and ornamental *Platanus*. Euphytica 126: 401–412

Bianchetti G, Baron C, Carrillo A, Berardocco S, Marnet N, Wagner M-H, Demilly D, Ducournau S, Manzanares-Dauleux MJ, Le Caherec F, Buitink J, Nesi N (2021) Dataset for the metabolic and physiological characterization of seeds from oilseed rape (*Brassica napus* L.) plants grown under single or combined effects of drought and clubroot pathogen *Plasmodiophora brassicae*. Data Brief 37: 107247

Bisba A, Petropoulou Y, Manetas Y (1997) The transiently pubescent young leaves of plane (*Platanus orientalis*) are deficient in photodissipative capacity. Physiol Plant 101: 373–378

Blanco V, Zoffoli JP, Ayala M (2021) Eco-physiological response, water productivity and fruit quality of sweet cherry trees under high tunnels. Sci Hortic 286: 110180

Bogeat-Triboulot M-B, Brosché M, Renaut J, Jouve L, Le Thiec D, Fayyaz P, Vinocur B, Witters E, Laukens K, Teichmann T, Altman A, Hausman J-F, Polle A, Kangasjärvi J, Dreyer E (2007) Gradual soil water depletion results in reversible changes of gene expression, protein profiles, ecophysiology, and growth performance in *Populus euphratica*, a poplar growing in arid regions. Plant Physiol 143: 876–892

Calfapietra C, Peñuelas J, Niinemets Ü (2015) Urban plant physiology: adaptation-mitigation strategies under permanent stress. Trends Plant Sci 20: 72–75

Caplan JS, Galanti RC, Olshevski S, Eisenman SW (2019) Water relations of street trees in green infrastructure tree trench systems. Urban For Urban Green 41: 170–178

Carraro E, Di Iorio A (2022) Eligible strategies of drought response to improve drought resistance in woody crops: a mini-review. Plant Biotechnol Rep 16: 265–282

Carrington Y, Guo J, Le CH, Fillo A, Kwon J, Tran LT, Ehlting J (2018) Evolution of a secondary metabolic pathway from primary metabolism: shikimate and quinate biosynthesis in plants. Plant J 95: 823–833

Cassab GI, Eapen D, Campos ME (2013) Root hydrotropism: An update. Am J Bot 100: 14–24

Cerovic ZG, Masdoumier G, Ghozlen NB, Latouche G (2012) A new optical leaf-clip meter for simultaneous non-destructive assessment of leaf chlorophyll and epidermal flavonoids. Physiol Plant 146: 251–260

Cui B, Wang X, Su Y, Gong C, Zhang D, Ouyang Z, Wang X (2022) Responses of tree growth, leaf area and physiology to pavement in *Ginkgo biloba* and *Platanus orientalis*. Front Plant Sci 13:

Czaja M, Kołton A, Muras P (2020) The complex issue of urban trees-Stress factor accumulation and ecological service possibilities. Forests 11: 932

David AAJ, Boura A, Lata J-C, Rankovic A, Kraepiel Y, Charlot C, Barot S, Abbadie L, Ngao J (2018) Street trees in Paris are sensitive to spring and autumn precipitation and recent climate changes. Urban Ecosyst 21: 133–145

Dellero Y, Heuillet M, Marnet N, Bellvert F, Millard P, Bouchereau A (2020) Sink/Source Balance of Leaves Influences Amino Acid Pools and Their Associated Metabolic Fluxes in Winter Oilseed Rape (*Brassica napus* L.). Metabolites 10: 150

Dellero Y, Jossier M, Bouchereau A, Hodges M, Leport L (2021) Leaf Phenological Stages of Winter Oilseed Rape (*Brassica napus* L.) Have Conserved Photosynthetic Efficiencies but Contrasted Intrinsic Water Use Efficiencies at High Light Intensities. Front Plant Sci 12: 659439

Dervishi V, Fleckenstein C, Rahman MA, Pauleit S, Ludwig F, Pretzsch H, Rötzer T (2023) Trees in planters – Growth, structure and ecosystem services of *Platanus x hispanica* and *Tilia cordata* and their reaction to soil drought. Urban For Urban Green 86: 128024

Esperon-Rodriguez M, Tjoelker MG, Lenoir J, Baumgartner JB, Beaumont LJ, Nipperess DA, Power SA, Richard B, Rymer PD, Gallagher RV (2022) Climate change increases global risk to urban forests. Nat Clim Chang 12: 950–955

Fàbregas N, Fernie AR (2019) The metabolic response to drought. J Exp Bot 70: 1077–1085

Farquhar GD, Hubick KT, Condon AG, Richards RA (1989) Carbon Isotope Fractionation and Plant Water-Use Efficiency,. Stable Isotopes in Ecological Research, Ecological Studies, Rundel, P.W., Ehleringer, J.R., Nagy, K.A. (Eds Ed. Springer, NY

Farquhar GD, O'Leary MH, Berry JA (1982) On the Relationship Between Carbon Isotope Discrimination and the Intercellular Carbon Dioxide Concentration in Leaves. Funct Plant Biol 9: 121–137

Franceschi E, Moser-Reischl A, Honold M, Rahman MA, Pretzsch H, Pauleit S, Rötzer T (2023) Urban environment, drought events and climate change strongly affect the growth of common urban tree species in a temperate city. Urban For Urban Green 88: 128083

Gatto E, Buccolieri R, Perronace L, Santiago JL (2021) The challenge in the management of historic trees in urban environments during climate change: the case of Corso Trieste (Rome,Italy). Atmosphere 12: 500

Genty B, Briantais J-M, Baker NR (1989) The relationship between the quantum yield of photosynthetic electron transport and quenching of chlorophyll fluorescence. Biochim Biophys Acta 990: 87–92

Gillner S, Korn S, Hofmann M, Roloff A (2017) Contrasting strategies for tree species to cope with heat and dry conditions at urban sites. Urban Ecosyst 20: 853–865

Gillner S, Korn S, Roloff A (2015) Leaf-gas exchange of five tree species at urban street sites. Arbor Urban For 41: 113–124

Gritsunov A, Peek J, Diaz Caballero J, Guttman D, Christendat D (2018) Structural and biochemical approaches uncover multiple evolutionary trajectories of plant quinate dehydrogenases. Plant J 95: 812–822

Guicherd P, Peltier JP, Gout E, Bligny R, Marigo G (1997) Osmotic adjustment in *Fraxinus excelsior* L.: malate and mannitol accumulation in leaves under drought conditions. Trees 11: 155–161

Heath RL, Packer L (1968) Photoperoxidation in isolated chloroplasts. I. Kinetics and stoichiometry of fatty acid peroxidation. Arch Biochem Biophys 125: 189–198

Hilbert D, Roman L, Koeser A, Vogt J, Van Doorn N (2019) Urban Tree Mortality: A Literature Review. Arbor Urban For 45:

Hirsch M, Böddeker H, Albrecht A, Saha S (2023) Drought tolerance differs between urban tree species but is not affected by the intensity of traffic pollution. Trees 37: 111–131

Ju R-T, Gao L, Wei S-J, Li B (2017) Spring warming increases the abundance of an invasive specialist insect: links to phenology and life history. Sci Rep 7: 14805

Kjelgren R, Montague T (1998) Urban tree transpiration over turf and asphalt surfaces. Atmos Environ 32: 35–41

Lang K (2010) Microsatellite development in *Platanus* for documenting gene flow among species. Thesis in Biological Sciences. California State University, Chico

Laoué J, Fernandez C, Ormeño E (2022) Plant flavonoids in Mediterranean species: a focus on flavonols as protective metabolites under climate stress. Plants 11: 172

Larondelle N, Lauf S (2016) Balancing demand and supply of multiple urban ecosystem services on different spatial scales. Ecosyst Serv 22: 18–31

Lawrence AB, Escobedo FJ, Staudhammer CL, Zipperer W (2012) Analyzing growth and mortality in a subtropical urban forest ecosystem. Landscape and Urban Planning 104: 85–94

Lunn JE, Delorge I, Figueroa CM, Van Dijck P, Stitt M (2014) Trehalose metabolism in plants. Plant J 79: 544–567

Macieira BPB, Locosselli GM, Buckeridge MS, Jardim VC, Krottenthaler S, Anhuf D, Helle G, Cuzzuol GRF, Ceccantini G (2021) Will climate change shift carbon allocation and stem hydraulics? Insights on a systemic view of carbon- and water-related wood traits in an anysohydric tropical tree species (*Hymenaea courbaril*, Leguminosae). Ecol Indic 128: 107798

Magné C, Larher F (1992) High sugar content of extracts interferes with colorimetric determination of amino acids and free proline. Anal Biochem 200: 115–118

Marchin RM, Esperon-Rodriguez M, Tjoelker MG, Ellsworth DS (2022) Crown dieback and mortality of urban trees linked to heatwaves during extreme drought. Sci Total Env 850: 157915

Monshausen GB, Gilroy S (2009) The exploring root—root growth responses to local environmental conditions. Curr Opin Plant Biol 12: 766–772

Montwé D, Hacke U, Schreiber SG, Stanfield RC (2019) Seasonal vascular tissue formation in four boreal tree species with a focus on callose deposition in the phloem. Front For Glob Change 2:

Morton CM, Gruszka P (2008) AFLP assessment of genetic variability in old vs. new London plane trees (*Platanus × acerifolia*). J Hortic Sci Biotech 83: 532–537

Mukhamedova SN, Abdullaeva MM, Levitskaya YV (2022) Seasonal dynamics of the main markers of stress in *Platanus orientalis* leaves in the conditions of the urban environment semiaride zone. Am J Agric Res 4: 1–6

Naor A (1998) Relations between leaf and stem water potentials and stomatal conductance in three field-grown woody species. J Hortic Sci Biotech 73: 431–436

Paris city (2023) Guide des essences de la ville de Paris. https://opendata.paris.fr/

Parri S, Romi M, Hoshika Y, Giovannelli A, Dias MC, Piritore FC, Cai G, Cantini C (2023) Morpho-physiological responses of three italian olive tree (*Olea europaea* L.) cultivars to drought stress. Horticulturae 9: 830

Pires MV, Pereira Júnior AA, Medeiros DB, Daloso DM, Pham PA, Barros KA, Engqvist MKM, Florian A, Krahnert I, Maurino VG, Araújo WL, Fernie AR (2016) The influence of alternative pathways of respiration that utilize branched-chain amino acids following water shortage in Arabidopsis. Plant Cell Environ 39: 1304–1319

Prislan P, Gričar J, De Luis M, Smith KT, Čufar K (2013) Phenological variation in xylem and phloem formation in *Fagus sylvatica* from two contrasting sites. Agric For Meteorol 180: 142–151

R Core Team (2023) R: A Language and Environment for Statistical Computing. https://www.R-project.org

Rahman MA, Fleckenstein C, Dervishi V, Ludwig F, Pretzsch H, Rötzer T, Pauleit S (2023) How good are containerized trees for urban cooling? Urban For Urban Green 79: 127822

Ribeiro J, Silva V, Aires A, Carvalho R, Barros L, Gaivão I, Igrejas G, Poeta P (2022) <i>Platanus hybrida<:i>'s phenolic profile, antioxidant power, and antibacterial activity against methicillin-resistant *Staphylococcus aureus* (MRSA). Horticulturae 8: 243

Rinaldi R, Cafasso D, Strumia S, Cristaudo A, Sebastiani F, Fineschi S (2019) The influence of a relict distribution on genetic structure and variation in the Mediterranean tree, *Platanus orientalis*. AoB Plants 11:

Ristic Z, Bukovnik U, Prasad PVV (2007) Correlation between heat stability of thylakoid membranes and loss of chlorophyll in winter wheat under heat stress. Crop Sci 47: 2067–2073

Roman LA, Scatena FN (2011) Street tree survival rates: Meta-analysis of previous studies and application to a field survey in Philadelphia, PA, USA. Urban For Urban Green 10: 269–274

Roy S, Byrne J, Pickering C (2012) A systematic quantitative review of urban tree benefits, costs, and assessment methods across cities in different climatic zones. Urban For Urban Green 11: 351–363

Santana-Vieira DDS, Freschi L, Almeida LA da H, Moraes DHS de, Neves DM, Santos LM dos, Bertolde FZ, Soares Filho W dos S, Coelho Filho MA, Gesteira A da S (2016) Survival strategies of citrus rootstocks subjected to drought. Sci Rep 6: 38775

Sanusi R, Livesley SJ (2020) London Plane trees (*Platanus x acerifolia*) before, during and after a heatwave: Losing leaves means less cooling benefit. Urban For Urban Green 54: 126746

Schädel C, Blöchl A, Richter A, Hoch G (2010) Quantification and monosaccharide composition of hemicelluloses from different plant functional types. Plant Physiol Biochem 48: 1–8

Semel Y, Schauer N, Roessner U, Zamir D, Fernie AR (2007) Metabolite analysis for the comparison of irrigated and non-irrigated field grown tomato of varying genotype. Metabolomics 3: 289–295

Sengupta S, Mukherjee S, Basak P, Majumder AL (2015) Significance of galactinol and raffinose family oligosaccharide synthesis in plants. Front Plant Sci 6: 656

Sherman AR, Kane B, Autio WA, Harris JR, Ryan HDP (2016) Establishment period of street trees growing in the Boston, MA metropolitan area. Urban For Urban Green 19: 95–102

Sofo A, Dichio B, Xiloyannis C, Masia A (2004) Effects of different irradiance levels on some antioxidant enzymes and on malondialdehyde content during rewatering in olive tree. Plant Sci 166: 293–302

Tan X, Hirabayashi S, Shibata S (2021) Estimation of ecosystem services provided by street trees in Kyoto, Japan. Forests 12: 311

Tattini M, Loreto F, Fini A, Guidi L, Brunetti C, Velikova V, Gori A, Ferrini F (2015) Isoprenoids and phenylpropanoids are part of the antioxidant defense orchestrated daily by drought-stressed *Platanus × acerifolia* plants during Mediterranean summers. New Phytol 207: 613–626

Tello ML, Redondo C, Mateo-Sagasta E (2000) Health Status of Plane Trees (*Platanus spp.*) in Spain. Arbor Urban For 26: 246–254

Tubby KV, Webber JF (2010) Pests and diseases threatening urban trees under a changing climate. Forestry 83: 451–459

Turner NC (2018) Turgor maintenance by osmotic adjustment: 40 years of progress. J Exp Bot 69: 3223–3233

Verslues PE, Sharma S (2010) Proline metabolism and its implications for plant-environment interaction. The Arabidopsis Book e0140.

Whitlow T, Bassuk N, Reichert D (1992) A 3-year study of water relations of urban street trees. J Appl Ecol 29: 436–450

Winkel-Shirley B (2002) Biosynthesis of flavonoids and effects of stress. Curr Opin Plant Biol 5: 218–223

Xiong S, Wang Y, Chen Y, Gao M, Zhao Y, Wu L (2022) Effects of drought stress and rehydration on physiological and biochemical properties of four Oak species in China. Plants 11: 679

Xu Y, Fu X (2022) Reprogramming of Plant Central Metabolism in Response to Abiotic Stresses: A Metabolomics View. Int J Mol Sci 23: 5716

Xu Y, Wang G, Cao F, Zhu C, Wang G, El-Kassaby YA (2014) Light intensity affects the growth and flavonol biosynthesis of Ginkgo (*Ginkgo biloba* L.). New Forests 45: 765–776

Yu Z, Dong W, Teixeira da Silva JA, He C, Si C, Duan J (2021) Ectopic expression of DoFLS1 from *Dendrobium officinale* enhances flavonol accumulation and abiotic stress tolerance in *Arabidopsis thaliana*. Protoplasma 258: 803–815

Zhang Y, Luan Q, Jiang J, Li Y (2021) Prediction and Utilization of Malondialdehyde in Exotic Pine Under Drought Stress Using Near-Infrared Spectroscopy. Front Plant Sci 12:

Zheng Y, Cabassa-Hourton C, Planchais S, Crilat E, Clément G, Dacher M, Durand N, Bordenave-Jacquemin M, Guivarc'h A, Dourmap C, Carol P, Lebreton S, Savouré A (2023) Pyrroline-5-carboxylate dehydrogenase is an essential enzyme for proline dehydrogenase function during dark-induced senescence in *Arabidopsis thaliana*. Plant Cell Environ 46: 901–917

Supporting information

4 supplemental tables and 8 supplemental figures

Supporting information

Claude et al., The isohydric strategy of *Platanus × hispanica* tree shapes its response to drought in an urban environment.

4 supplemental tables and 8 supplemental figures

Table S1: Table of reference trees from "Muséum National d'Histoire Naturelle" (MNHN) in Paris ("Jardin des Plantes") and in Versailles-Chèvreloup Arboretum (78150 Rocquencourt, France) used for genetic analysis.

MNHN garden	*species*	MNHN ref.	remarks
Jardin des Plantes	*Platanus × hispanica 'Densicoma'*	13075	exceptional tree
Jardin des Plantes	*Platanus × hispanica*	13258	exceptional tree
Jardin des Plantes	*Platanus × hispanica*	13259	
Jardin des Plantes	*Platanus orientalis*	14263	« Buffon » tree (1785)
Jardin des Plantes	*Platanus × hispanica*	280	20-25 years old
Jardin des Plantes	*Platanus × hispanica*	273	130 years old
Chèvreloup Arboretum	*Platanus occidentalis*	ARB31455	planted in 1995

Table S2: Primers sequences used for microsatellite analyses.

Name [ref]	Primer sequence	Amplicon Size (bp)	Dye	Emission (nm)
plms17 [1]	F : GGAGAAAGAGAAGAAGGAGAAAAA R : AGGGTCTTGGTCGTGATTTG	219-239	PET	595
plms29 [1]	F : GCCCATTAGATGGGTTGAAA R : AGCGAATCCATGTGCCTAAT	208-224	6-FAM	520
plms68 [1]	F : TGAATCCCAAAAGGCAAAAA R : AAACACCCAATCCGGTCTAC	170-184	6-FAM	520
plms109 [1]	F : TGATGACAAATACTCAGGGAAA R : CGATAGCCAAAAGCGAAAGA	121-145	VIC	554
plms113 [1]	F : GGCAAGCCAGGATTTAGTTG R : CGGGATAAGAGTTTGTTGAGTTG	202-228	NED	575
plms122 [1]	F : CTTCTGTGCTTGTGCCTCAC R : CTTTGCACCAATGTGCCTTA	223-225	VIC	554
plms130 [1]	F : TACCACACCAACGTCCTTCC R : ACCCTCTCAAATATGCCAATTA	208-214	PET	595
plms176 [1]	F : AACAGCAAAACAGCCCACTC R : AAACCAGCCAATCCAATTCC	269-275	NED	575
11FAM [2]	F : TCGGTGGTCGAATTCATCCC R : GAAAGCATGCCGATGTGGG	202-236	PET	595
PI2A [2]	F : GAGGGAAGGATTGCCCAGTTG R : CTATCAACTTCTAGATCCCTAG	332-354	NED	575

(1) Lang (2010)
(2) Rinaldi et al. (2019)

Table S3: M**icrosatellite analysis results: sizes of amplicons obtained with specific primers**. plm29' and plm 113' corresponded to alleles amplified with plm39 and plm113 respectively but less frequent than the first ones. The grey color refers to identical allele combination. nd : missing data. 0 : no amplicon.

primers		plms17	plms29	plms29'	plms68	plms109	plms113	plms113'	plms122	plms130	plms176	11FAM	PI2A
exp. trees	1A	235, 470	224, 217	0	191, 191	140, 140	218, 224	0	225, 225	206, 206	262, 266	208, 216	289, 289
	1B	235, 470	224, 224	0	191, 191	140, 140	218, 224	0	225, 225	206, 206	262, 266	208, 216	289, 289
	2A	235, 470	224, 217	0	191, 191	140, 140	218, 224	0	225, 225	206, 206	262, 266	nd	289, 289
	2B	235, 470	224, 217	206, 206	191, 191	140, 140	218, 224	0	225, 225	206, 206	262, 266	208, 216	289, 289
	3A	235, 470	224, 217	190, 190	191, 191	nd	218, 224	0	225, 225	206, 206	262, 266	208, 216	289, 289
	3B	235, 470	224, 217	0	191, 191	nd	**nd**	nd	225, 225	206, 206	262, 266	nd	nd
	4A	235, 470	224, 224	0	191, 191	140, 140	218, 224	0	225, 225	206, 206	262, 266	208, 216	289, 289
	4B	235, 470	224, 224	0	191, 191	140, 140	218, 224	0	225, 225	206, 206	262, 266	208, 216	289, 289
	5A	235, 470	nd	nd	191, 191	140, 140	218, 224	298, 304	nd	nd	nd	208, 216	289, 289
	5B	235, 470	224, 217	0	191, 191	140, 140	218, 224	0	nd	206, 206	262, 266	208, 216	289, 289
	6A	235, 470	224, 224	0	191, 191	140, 140	218, 224	0	225, 225	206, 206	262, 266	nd	nd
	6B	235, 470	224, 224	0	191, 191	140, 140	218, 224	0	225, 225	206, 206	262, 266	208, 216	289, 289
	7A	235, 470	224, 217	0	191, 191	nd	218, 224	0	225, 225	206, 206	262, 266	208, 216	0
	7B	235, 470	224, 217	0	191, 191	nd	218, 224	0	225, 225	206, 206	262, 266	nd	nd
	Adult tree	235, 470	224, 217	206, 206	191, 191	140, 140	218, 224	0	225, 225	206, 206	262, 266	208, 208	289, 289
ref. trees	*P. × hispanica 280*	235, 235	0	208, 208	191, 118	118, 118	218, 224	298, 304	225, 232	211, 213	272, 266	208	118, 118
	P. × hispanica 273	235, 470	224, 224	0	191, 191	nd	218, 224	298, 304	225, 225	206, 206	262, 266	208, 216	nd
	P. × hispanica 'Densicoma' 13075	235, 470	224, 224	0	191, 191	140, 140	218, 224	0	225, 225	206, 206	262, 266	208, 216	nd
	P. × hispanica 13259	235, 470	224, 224	0	191, 118	118, 140	218, 224	298	225, 225	206, 206	262, 266	208, 216	nd
	P. × hispanica 13258	235, 470	224, 217	208, 208	191, 118	118, 140	218, 224	298, 304	225, 225	nb	262, 266	140, 140	nd
	P. orientalis "Buffon" 14263	235, 470	217, 217	208, 208	191, 118	118, 140	218, 224	0	225, 225	nd	262, 266	208, 218	289, 289
	P. occidentalis ARB31455	235, 235	224, 224	0	185, 185	140, 140	218, 224	298, 304	225, 225	206, 206	262, 266	216, 216	309, 309

Table S4: **Quantification of the *Platanus* lace bug (*Corythucha ciliate*) density and evolution of general appearance of the leaves**. One branch per tree was followed every 2 weeks.

Date	Treatment	***Corythucha ciliata* density (dm^{-2}_{leaves})**	**Leaves with necrosis (%)**	**Leaves with chlorosis (%)**	**Emerging leaves (%)**	**Yellowing leaves (%)**
Week (17)	Control	47 ± 12.8	43.7 ± 10.4	49.7 ± 13.7	0 ± 0	0 ± 0
	Drought	31 ± 9.1	47.1 ± 5.6	67.2 ± 9.9	0 ± 0	0 ± 0
Week (19)	Control	23 ± 4.1	34.1 ± 7.3	67.9 ± 14.2	0 ± 0	0 ± 0
	Drought	44.6 ± 10.4 ●	41.8 ± 2.3	78.5 ± 4.3	0 ± 0	0 ± 0
Week (20)	Control	4.3 ± 1.2	40.2 ± 4.3	82.7 ± 3.2	5.5 ± 0.7	0 ± 0
	Drought	9.3 ± 3.2	37.1 ± 2.4	76.1 ± 1.9	11.2 ± 1.6 **	0 ± 0
Week (22)	Control	3 ± 1.1	52.3 ± 1.1	79.8 ± 3.2	7.5 ± 1.8	3.4 ± 1.6
	Drought	2.7 ± 1.4	47.6 ± 3.1	69.7 ± 2.8 ●	8.9 ± 1.5	16 ± 2.5 **
Week (24)	Control	0.7 ± 0.7	50.9 ± 1.3	85.2 ± 1.8	1 ± 0.6	2.6 ± 1
	Drought	4.6 ± 3.3	79.9 ± 6.3 **	69.1 ± 14.5	0.5 ± 0.5	63.7 ± 12.4 **

Wilcoxon-Mann-Whitney test, *** p-value < 0.001, ** p-value < 0.01, * p-value < 0.05, • p-value < 0.1

Water withholding started on week 21

Fig. S1: Description of the study site. Location of the study site in Vitry/Seine (Paris suburb, France; **a**; map ©IGN, in the yard of University Paris Est Créteil (**b;** map ©Google). The red rectangle represents the young studied plane trees. (**c**) Map of the experimental setup with 14 London plane trees arranged in two rows (A & B) near a row of adult trees. (**d**) Picture of trees in June 2022. (**e**) total rainfall exclusion system (**f**) Specification of the substrate used.

a

b

c

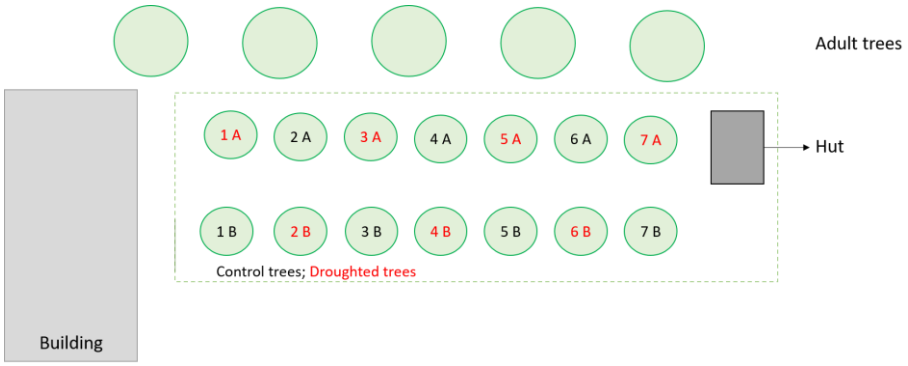

d

e

f The **substrate** used to fill the containers provided by Premier Tech (France) and composed of 25% of sieved topsoil, 15% of vegetable compost, 10% of composted horse manure, 13% of wood fiber, 15% of coconut fiber medium, 2% of clay and 20% of maritime pine bark (pH=6.2 ± 0.2; conductivity: ~0.90 mS cm^{-1}). A layer of clay balls for drainage was poured at the bottom on the containers and separated from the substrate with a geotextile.

Fig. S2: **Weekly extractable soil water content according to depth**. Filled triangles (▲)and circles (●) represent droughted trees and control trees, respectively. Symbols represent the weekly mean value (n= 6), with error bars representing the S.E.M. The symbol color corresponds to the watering, with blue and red indicating trees without or with water withholding, respectively.

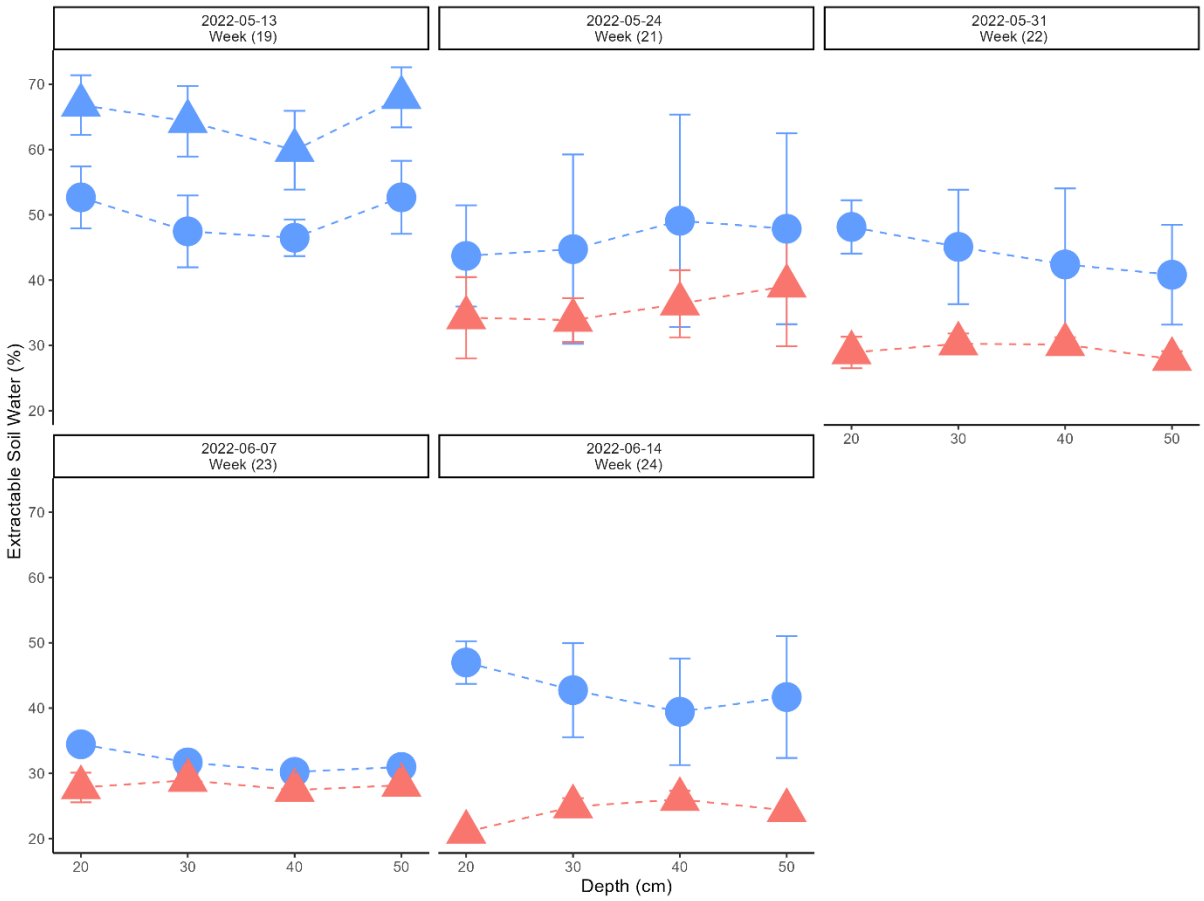

Fig. S3: **Allometric relation between the major vein length and projected area of *Platanus × hispanica* leaves**. Leaves (n= 368) from the 12 trees were collected and scanned. From the images, the projected leaf area and the length of the major leaf vein **(a)** were measured using the ImageJ software. These measurements allowed to obtain, for the major vein length, a relationship with the projected leaf area (**b**). The associated equation and the coefficient of determination (R^2) are mentioned in the graph.

a

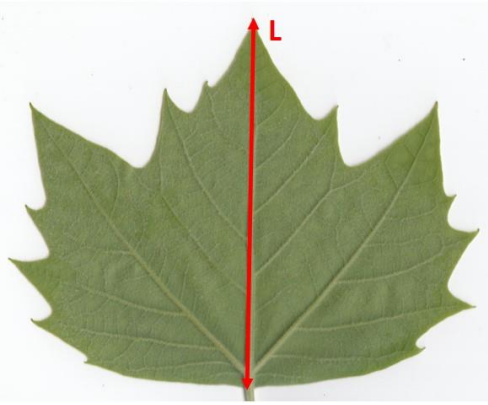

b

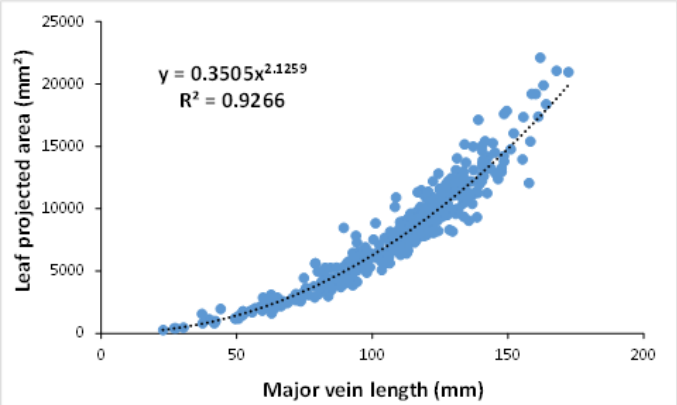

Fig. S4: Evolution of branch leaf surface over the experiment. (a) Relative leaf surface and (b) Relationship between branch leaf surface and the number of leaves. Parameter was determined on selected branches located at equivalent height. Relative leaf surface (a) was expressed relative to the maximal leaf surface (100 %) determined on week 22. For (b), light and dark symbols represent early and late weeks, respectively and the coefficient of determination (R^2) of the significant linear regression is indicated. Triangles (▲) with solid line and circles (●) with dashed line represent droughted trees and control trees, respectively. Small symbols represent individual trees while larger ones represent the weekly mean value (n=6), with vertical error bars representing the S.E.M. The symbol color corresponds to the watering, with blue and red indicating trees without or with water withholding, respectively. Significance of variations between weeks, in response to drought or the interaction of both factors are presented on the figure (linear mixed model followed by a type II ANOVA). Asterisks indicates significance differences between drought and control trees in the week (Tukey HSD post-hoc test, *** p-value < 0.001, ** p-value < 0.01, * p-value < 0.05, ● p-value < 0.1).

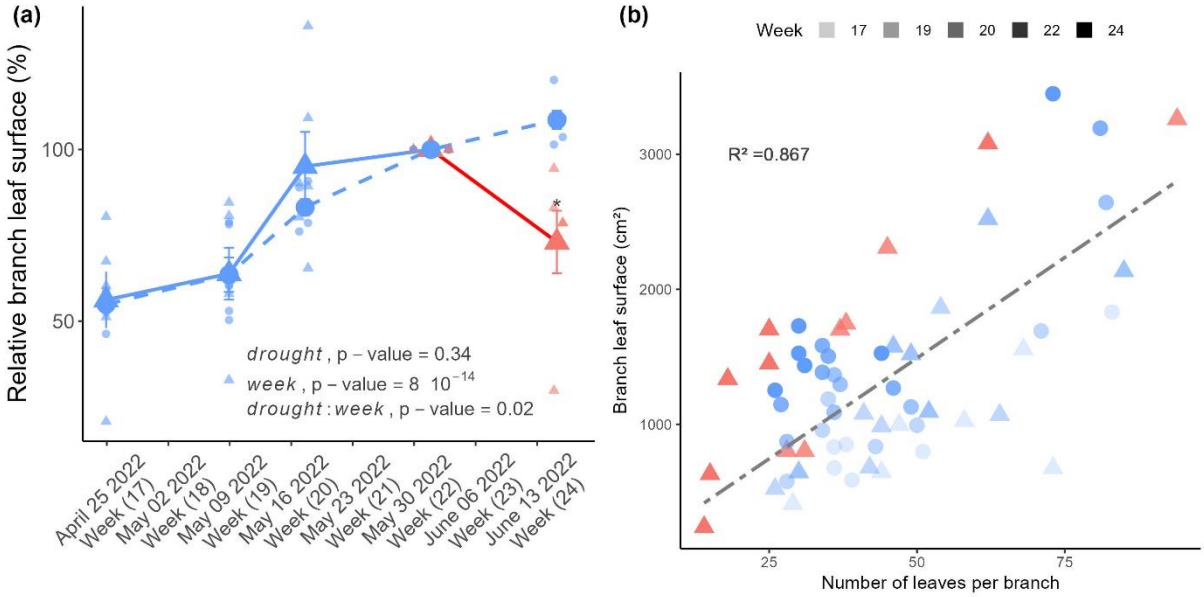

Fig. S5: **Evolution of conductance Gs measured by porometry.** Conductance was followed each week during the drought treatment during one day (2 or 3 measurement series per tree) each week. Triangles (▲) and circles (●) represent droughted trees and control trees, respectively. The symbol color corresponds to the watering, with blue and red indicating trees without or with water withholding, respectively. Line and interval represent the daily median and range (minimal and maximal) Gs value. The coefficient of determination (R^2) of the model and the p-value associated to the drought effect are mentioned in each graph.

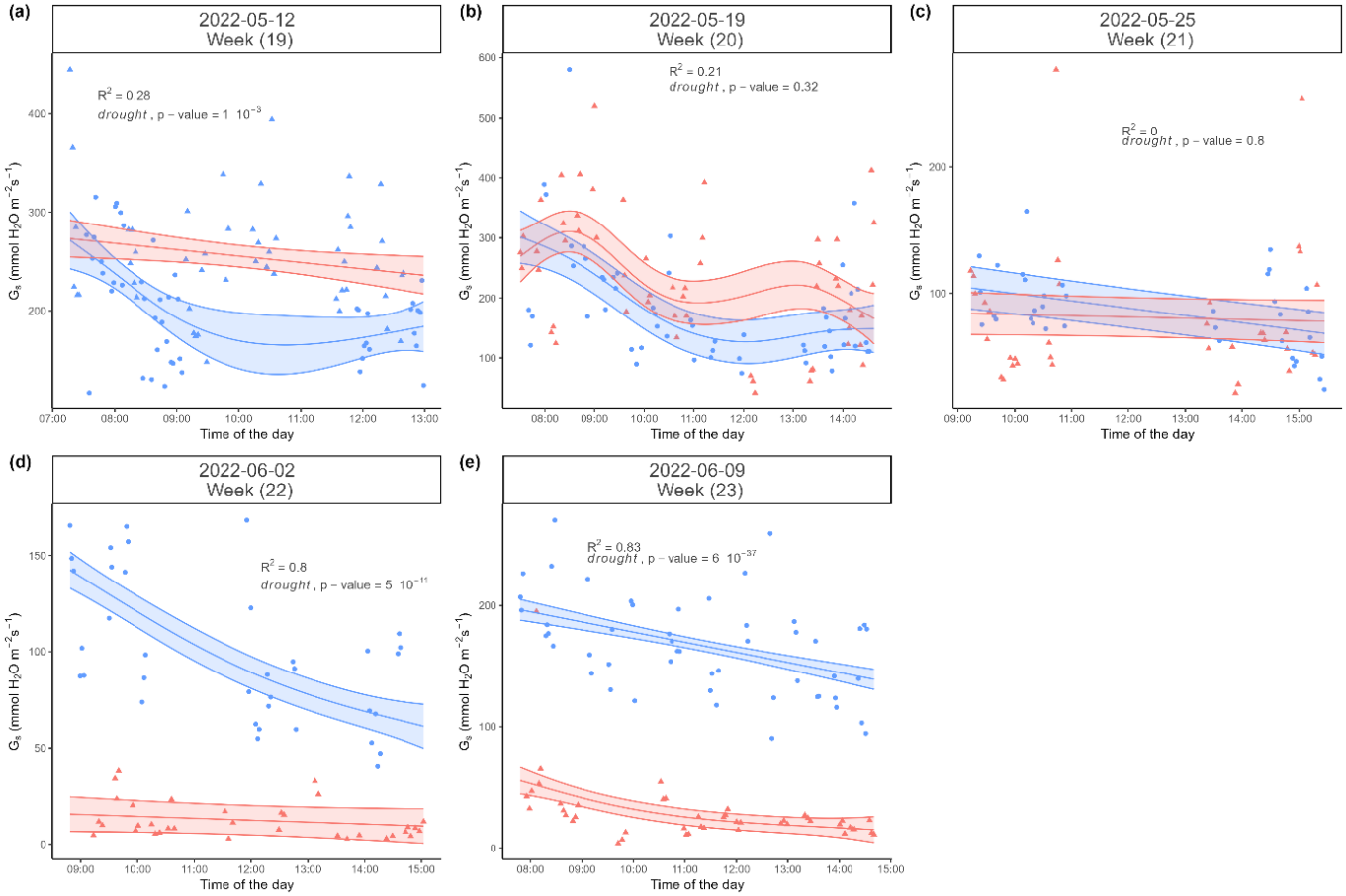

Fig. S6: **Targeted metabolome profiling**. Concentration in leaves (µmol. g^{-1}DW) of all metabolites analyzed. The color of the name of compound refers to its chemical class: organic acids in green, polyols in purple, sugars in blue, and amino acids in red. The results of the statistical tests are indicated above the square brackets, the first one for seasonality effect (control May vs control June), the second one for drought effect (control June vs drought June). ns: not significant; * significant (Wilcoxon-Mann-Whitney test; p-value<0.05). Points refers to outliers data.

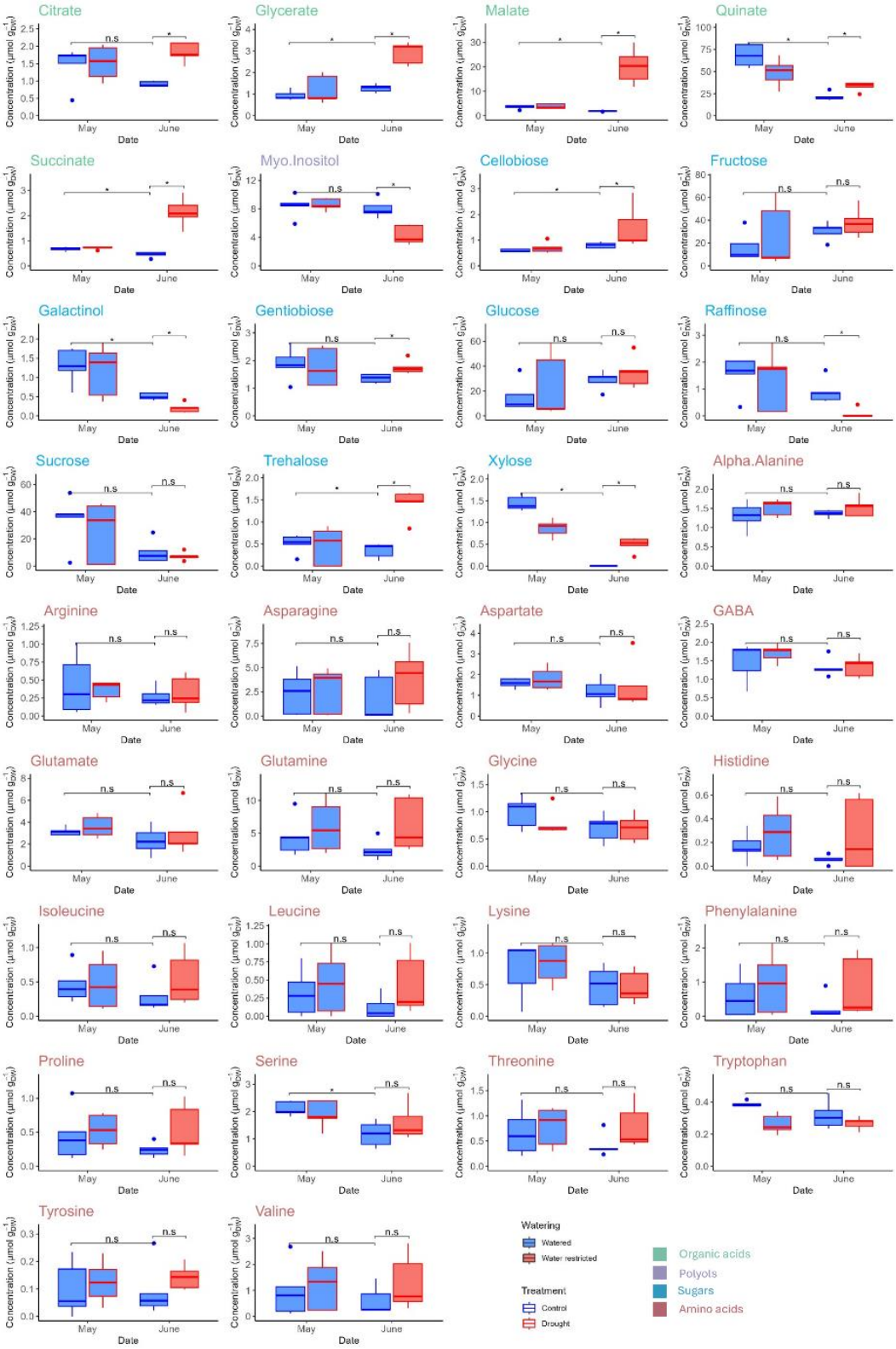

Fig. S7: Variables contribution to the (a) first and the (b) second dimension of the PCA presented in Fig. 6. The red dashed line indicates the expected average contribution (7.7 %).

(a)

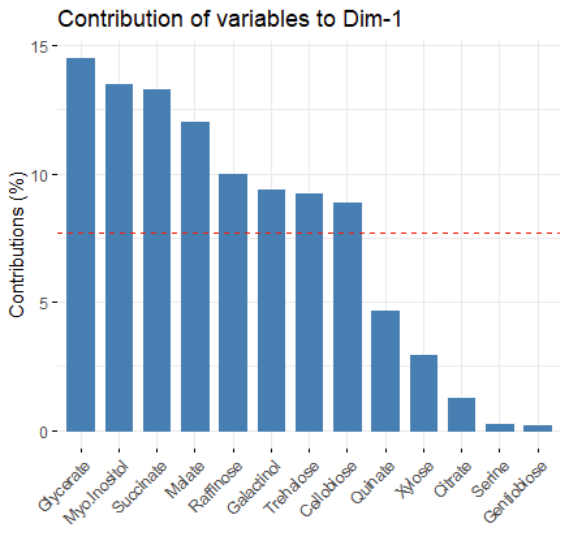

(b)

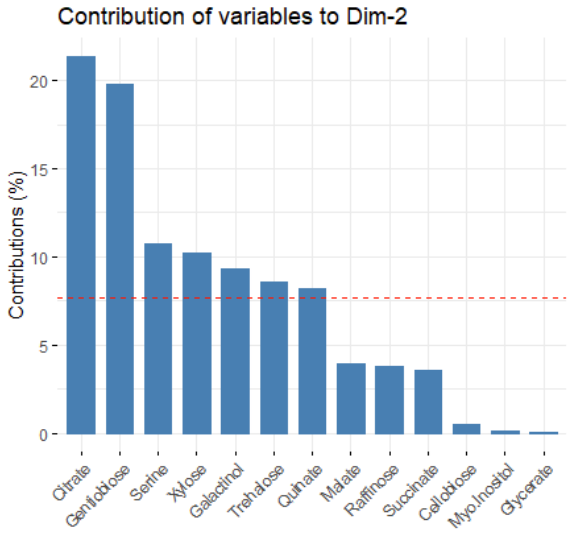

Fig. S8: Spearman's rank correlation between analysed metabolites. Positive correlations (rho > 0) are shown in red and negative correlations (rho < 0) are shown in blue. The size of the circle shows the correlation strength. The color of the name of compound refers to its chemical class.